Atmospheric Iron Deposition: Global Distribution, Variability, and Human Perturbations*

Natalie M. Mahowald,[1,2] Sebastian Engelstaedter,[1]
Chao Luo,[1] Andrea Sealy,[2] Paulo Artaxo,[3]
Claudia Benitez-Nelson,[4] Sophie Bonnet,[5]
Ying Chen,[6] Patrick Y. Chuang,[7] David D. Cohen,[8]
Francois Dulac,[9,10] Barak Herut,[11] Anne M. Johansen,[12]
Nilgun Kubilay,[13] Remi Losno,[10] Willy Maenhaut,[14]
Adina Paytan,[15] Joseph M. Prospero,[16]
Lindsey M. Shank,[12] and Ronald L. Siefert[17]

[1]Department of Earth and Atmospheric Sciences, Cornell University, Ithaca, New York 14853

[2]National Center for Atmospheric Research, Boulder, Colorado 80307;
email: mahowald@cornell.edu

[3]Instituto de Fisica, Universidade de Sao Paulo, Sao Paulo, 05508-900 SP, Brazil

[4]Department of Geological Science and Marine Science Program, University of South Carolina, Columbia, South Carolina 29208

[5]Laboratoire d'Océanographie de Villefranche, UMR 7093, BP 8-06238 Villefranche-sur-mer Cedex, France

[6]Trinity Consultants, Irvine, California 92618

[7]Department of Earth and Planetary Sciences, University of California, Santa Cruz, California 95064

[8]Australian Nuclear Science and Technology Organisation, Menai, 2234 NSW, Australia

[9]Laboratoire des Sciences du Climat et de l'Environnement, UMR 1572 CEA-CNRS-UVSQ, CEA Saclay, Gif-Sur-Yvette, France

[10]Laboratoire Interuniversitaire des Systèmes Atmosphériques, UMR 7583 CNRS-UP12-UP7, University of Paris 12, Créteil, France

[11]Israel Oceanographic and Limnological Research, National Institute of Oceanography, Haifa, Israel

[12]Department of Chemistry, Central Washington University, Ellensburg, Washington 98926

[13]Institute of Marine Sciences, Middle East Technical University, P.K. 28, Erdemli, Turkey

[14]Department of Analytical Chemistry, Institute for Nuclear Sciences, Ghent University, B-9000 Ghent, Belgium

[15]Institute for Marine Sciences, University of California, Santa Cruz, California 95064

[16]Rosenstiel School of Marine and Atmospheric Science, Marine and Atmospheric Chemistry, University of Miami, Miami, Florida 33149

[17]Chemistry Department, U.S. Naval Academy, Annapolis, Maryland 21402

Abstract

Atmospheric inputs of iron to the open ocean are hypothesized to modulate ocean biogeochemistry. This review presents an integration of available observations of atmospheric iron and iron deposition, and also covers bioavailable iron distributions. Methods for estimating temporal variability in ocean deposition over the recent past are reviewed. Desert dust iron is estimated to represent 95% of the global atmospheric iron cycle, and combustion sources of iron are responsible for the remaining 5%. Humans may be significantly perturbing desert dust (up to 50%). The sources of bioavailable iron are less well understood than those of iron, partly because we do not know what speciation of the iron is bioavailable. Bioavailable iron can derive from atmospheric processing of relatively insoluble desert dust iron or from direct emissions of soluble iron from combustion sources. These results imply that humans could be substantially impacting iron and bioavailable iron deposition to ocean regions, but there are large uncertainties in our understanding.

INTRODUCTION

The ocean is currently absorbing roughly one-third of the carbon dioxide emitted by human activity (e.g., Denman et al. 2007). Thus, understanding how ocean uptake of carbon dioxide will be modified in the upcoming century is an important issue for projecting future climate change. Iron is an essential micronutrient for ocean biota growth and the absence of iron has been linked to the existence of high-nutrient low-chlorophyll regions, as well as changes in the concentration of carbon dioxide on glacial-interglacial timescales (Martin 1990, Ridgwell & Watson 2002). Although controversial, nitrogen-fixing organisms in the ocean may have higher iron requirements than other phytoplankton (e.g., Falkowski et al. 1998, Mills et al. 2004), which would directly link iron and nitrogen biogeochemical cycles (e.g., Moore et al. 2004). Although sedimentary sources of iron are important as well (Lam et al. 2006), the atmospheric input plays a major role in open ocean regions (Fung et al. 2000). Thus, understanding atmospheric deposition of iron to the oceans and how humans may be perturbing deposition is an important question and the focus of this review.

Most atmospheric iron is carried in mineral aerosols, and previous reviews have focused on these aerosols (e.g., Duce & Tindale 1991, Mahowald et al. 2005). Here we look specifically at iron concentration and deposition observations, as well as datasets that can be used to estimate interannual variability in iron deposition to ocean regions. We include studies of the impact of combustion sources of iron, as well as consider desert dust and the potential human impacts on that desert dust iron source. We focus on changes in the iron cycle that have occurred over the past 100 years and are expected to occur into the future. New data and modeling studies have highlighted the potential for human perturbation to soluble or bioavailable iron (Guieu et al. 2005, Chuang et al. 2005, Sedwick et al. 2007, Luo et al. 2008). As we discuss below, large uncertainties remain in our understanding of the distribution, variability, and human impacts on iron and soluble iron deposition to the ocean.

IRON SOURCES AND DISTRIBUTION

Mineral aerosol sources of iron represent approximately 95% of the globally averaged atmospheric budget, with the remaining fraction attributed to industry, biofuels, and biomass burning (Luo et al. 2008). Mineral aerosols or desert dust are soil particles suspended in the atmosphere by strong winds. Mineral aerosol entrainment requires dry, unvegetated, and easily erodible soils (e.g., review by Mahowald et al. 2005). The largest source of iron comes from the North African deserts, and thus the largest deposition to the oceans occurs in the North Atlantic and Mediterranean downwind of the North African coast (e.g., Prospero 1996, Guerzoni et al. 1997). Varying amounts of iron can exist in soils and thus in mineral aerosols (Claquin et al. 1999, Hand et al. 2004), although data and models suggest that this variation leads to less than 50% of the differences in the amount of iron in the atmosphere or its deposition (Hand et al. 2004, Mahowald et al. 2005), and thus it is less than other uncertainties in the iron deposition budget, as discussed below. Other sources of iron have also been postulated. Volcanic eruptions can provide important episodic sources of iron (Duggen et al. 2007, Frogner et al. 2001). Johnson (2001) postulated the importance of extraterrestrial sources of iron, but these deposition estimates are lower than estimates from atmospheric processing or direct combustion estimates (discussed below).

Mineral aerosols and iron can be transported in the troposphere downwind for long distances (e.g., Prospero 1999, Grousset et al. 2003), and are removed by both wet and dry deposition processes (Seinfeld & Pandis 1998). Wet deposition occurs when aerosol particles are removed in precipitation events (entrained into the water drops either within or below the cloud). Dry deposition processes include turbulent deposition, in which random eddies force the particles to impact the ground, or gravitational settling, in which larger particles are removed owing to their density and size. Lifetimes of iron bearing aerosols are estimated to be between days (for large particles >2 μm) to weeks for smaller particles (e.g., Tegen & Fung 1994, Ginoux et al. 2001; Luo et al. 2008).

Global Distribution of Iron

The limited number of direct measurements of iron deposition (**Supplemental Table 1**; follow the **Supplemental Material link** from the Annual Reviews home page at **http://www.annualreviews.org**) makes it difficult to deduce iron distributions from iron deposition measurements. Others have reviewed the available mineral aerosol deposition datasets (e.g., Kohfeld & Harrison 2001, Tegen et al. 2002, Ginoux et al. 2001) (**Figure 1a**). Direct measurement of deposition on land or in ice cores provides good constraints on total mineral aerosol deposition [e.g., the dataset compiled in Ginoux et al. (2001) or Mahowald et al. (1999)], but deposition is measured directly at only a few sites. Observations of mineral aerosol deposition into the oceans in sediment traps or marine sediment cores (e.g., Kohfeld & Harrison 2001) are difficult to interpret. Sediment traps or marine sediment cores are influenced by the water column advection of the aerosols, and do not represent necessarily the deposition at the point of measurement (Siegel & Deuser 1997, Bory et al. 2002). Sediment trap fluxes are also variable in time and dependent on ocean productivity (Bory & Newton 2000), and indeed the dust can act as a ballast to enhance downward ocean fluxes (Francois et al. 2002). In addition, dust fluxes to sediment traps are often determined by differencing two large numbers (total fluxes from the biogenic organic components), which can lead to errors (e.g., Jickells et al. 1998). Furthermore, marine sediment core measurements have additional errors in calculating current dust flux as a result of problems in retrieving the top of the core as well as from uncertainties in the age models (deMenocal et al. 2000, Winckler et al. 2008). Thus, we do not show the marine sediment cores compiled in the dust indicators and records of terrestrial and marine paleoenvironments (DIRTMAP) dataset
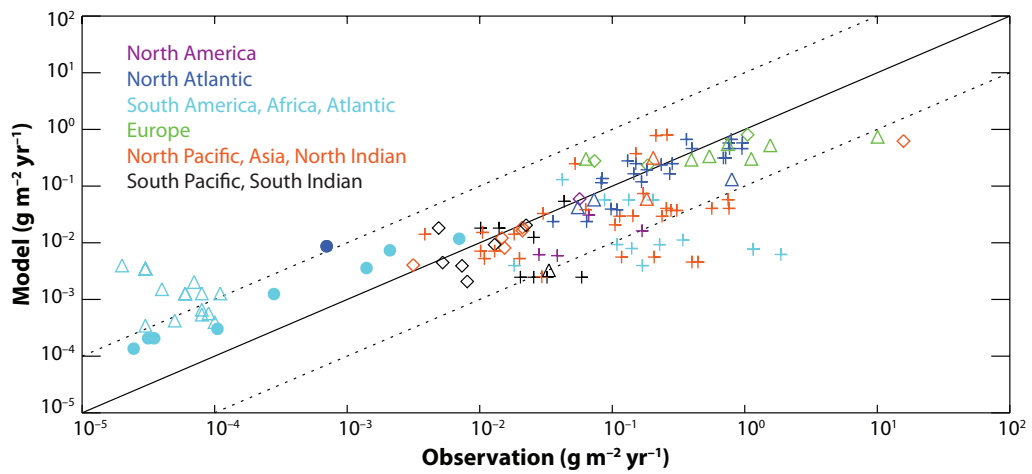
a Observed Fe

Fe (g m⁻² yr⁻¹)
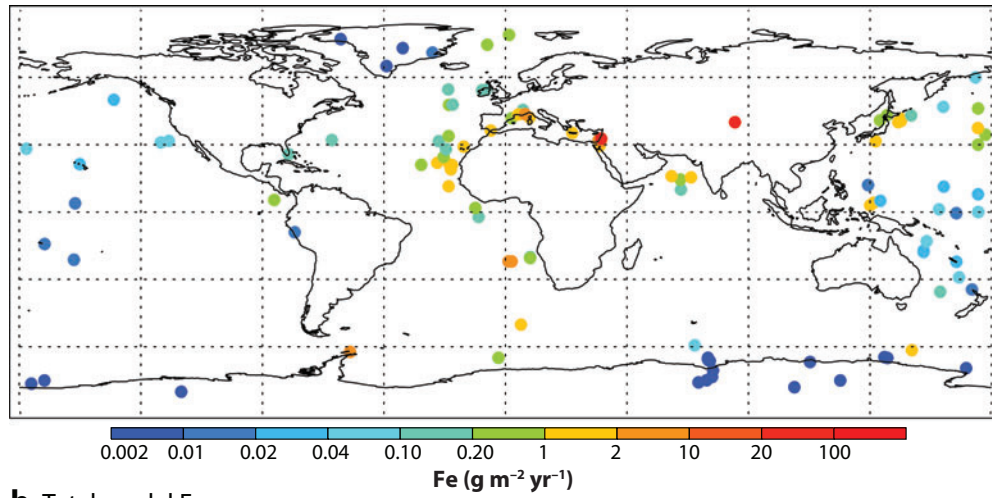
b Total model Fe
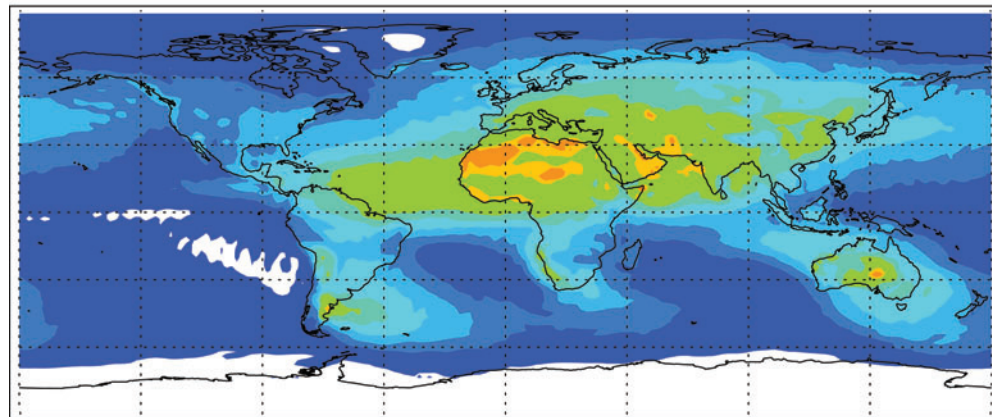
c Scatter diagram

(Kohfeld & Harrison 2001) in **Figure 1a**. In general **Figure 1a** demonstrates that more direct measurements of iron and/or dust deposition are much needed to improve our understanding of iron deposition.

Several high-quality datasets contain iron concentrations in aerosols less than 10 μm in size (total suspended particulate is shown for Tel-Shikmona, Erdemli, Meteor, and Aegaeo cruises). These data are compiled in **Supplemental Table 2** and shown in **Figure 2a** and include long-term monitoring stations and cruise tracks (where only one daily averaged measurement sample is available for each point on the graph). We also include data from stations and cruises where dust concentration was determined, assuming dust contains 3.5% iron (Taylor & McLennan 1985).

Another valuable tool in development for understanding iron deposition is the measurement of ocean iron and aluminum (e.g., Measures & Brown 1996, Dulac et al. 1996, Gehlen et al. 2003, Bergquist & Boyle 2006, Chase et al. 2006, Bonnet & Guieu 2006, Han et al. 2008). Unfortunately, iron is difficult to measure accurately at the low concentrations observed (e.g., Boyle et al. 2005, Johnson et al. 2007), but much more data should be available in the future because of large-scale sampling programs (e.g., **http://www.ldeo.columbia.edu/res/pi/geotraces/**). Ocean iron concentrations will necessarily include ocean advection of incoming atmospheric iron, but for understanding ocean iron and the importance of atmospheric inputs, these new datasets will be vitally important.

Aerosol Modeling

Because of the limitations in the amount of data available on the distribution of iron or desert dust, we often use models to extrapolate the limited data both in space and time. Aerosol modeling contains substantial uncertainties, but several models of mineral aerosol entrainment, transport, and deposition exist. The literature contains reviews of dust models (e.g., Tegen 2003, Mahowald et al. 2005) and model intercomparisons (e.g., Textor et al. 2006), as well as syntheses of available data (Miller et al. 2006). Currently only one published study includes combustion sources of iron (Luo et al. 2008).

Here we briefly review dust modeling, including entrainment, transport, and deposition, especially describing a model that is used below to extrapolate available observations. Long-range transport of dust particles is usually in the range smaller than 12 μm (D'Almeida 1986, Reid et al. 2003). Larger particles fall out of the atmosphere too quickly to be transported very far (e.g., Seinfeld & Pandis 1998). However, the atmospheric transport of giant aeolian quartz grains (>62.5 μm) has been suggested to occur more often than previously thought, although the mechanisms that facilitate large-sized grain transport are not understood (Dulac et al. 1992, Middleton et al. 2001, Reid et al. 2003). The emission of dust into the atmosphere shows a highly nonlinear relationship to changes in vegetation, soil moisture, soil size distribution, and atmospheric conditions. Any vegetation or surface soil moisture is likely to hold down the soil, making entrainment unlikely (e.g., Marticorena & Bergametti 1995). The relationship between soil size distribution and dust entrainment is more complicated. Although the availability of small particles is required

← ---

Figure 1

Deposition of iron (g m^{-2} year^{-1}) in (*a*) the observations, (*b*) a model, and (*c*) a scatter plot comparison. For panel (*c*), ice core records are shown as filled-in circles [compiled in Mahowald et al. (1999)], the deposition compilation from Ginoux et al. (2001) is shown as triangles, and the sediment trap compilation in Tegen et al. (2002) is shown as plus symbols. New deposition data compiled for this study are shown as triangles and appear in **Supplemental Table 1**.

a Observation
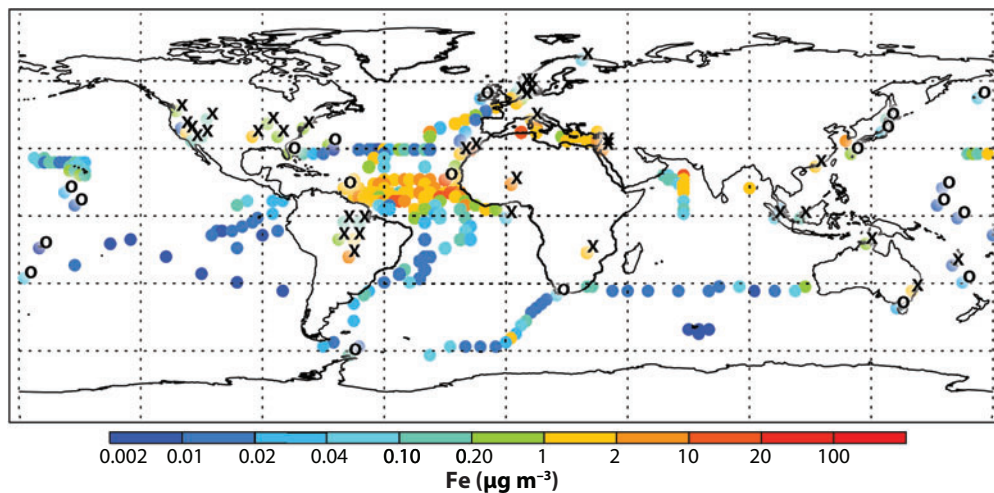
b Total model
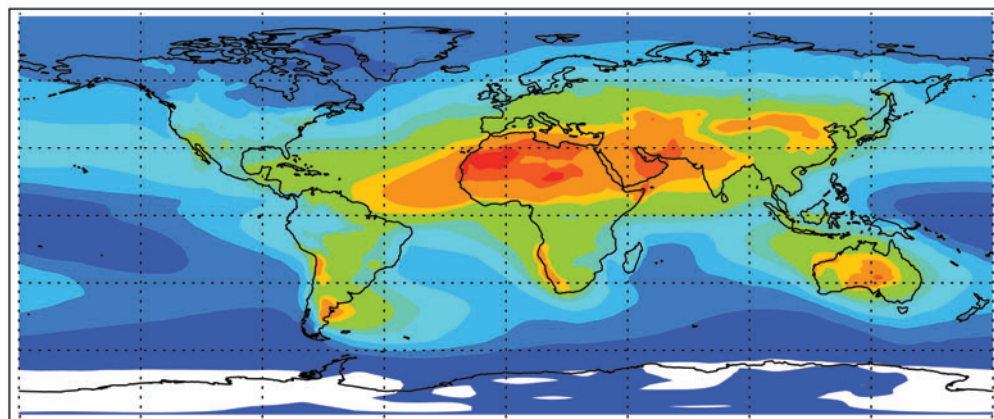
c Scatter diagram
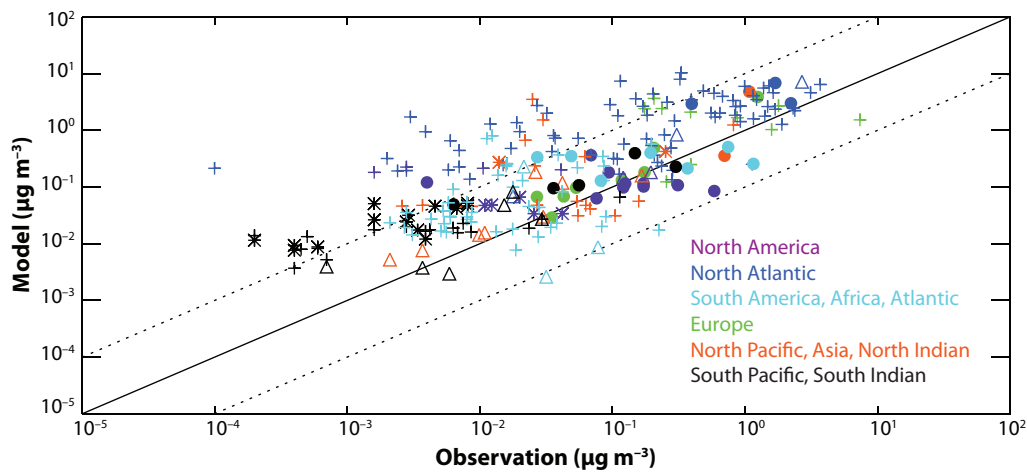
for long-range transport, small particles are not directly entrained by the wind because of the large cohesive forces that bind these particles. Larger particles (>60 μm) begin moving with the wind (saltation) and these particles entrain or break apart into smaller particles (e.g., Zender et al. 2003). A small fraction of the particles, however, are entrained into the free atmosphere, and become dust aerosols (e.g., Marticorena & Bergametti 1995). The source term for entrainment of dust into the atmosphere depends on wind speed at the surface (friction velocity), and increases rapidly with higher wind speeds (e.g., Marticorena & Bergametti 1995). These higher surface winds need not be the mean winds in an area or front synoptic systems, but rather wind gusts because of strong surface heating (Miller et al. 2004, Luo et al. 2004, Engelstaedter & Washington 2007). Because of the highly nonlinear nature of dust sources, small regions possibly represent the source of most of the dust to the atmosphere (Gillette 1999, Prospero et al. 2002, Mahowald et al. 2005).

As discussed above, dust is removed by dry or wet deposition, and both processes are parameterized in the models (e.g., Seinfeld & Pandis 1998, Rasch et al. 2000). Dust is transported with the mean large-scale winds as well as in vertical mixing from dry or moist convection. Models can provide us with daily averaged deposition (or higher resolution) at any location globally, and have been evaluated for mean distribution (e.g., Tegen & Fung 1994, Ginoux et al. 2001), interannual variability (Mahowald et al. 2003, Ginoux et al. 2004), and daily variability (e.g., Mahowald et al. 2002, Hand et al. 2004). Dust models are able to accurately follow the transport of specific dust events for many days (e.g., Ginoux et al. 2001; Grousset et al. 2003).

Next we focus on one set of model studies used to extrapolate data (Luo et al. 2003, 2005, 2008; Mahowald et al. 2003; Hand et al. 2004). Comparisons of modeled deposition to data (**Figure 1***b* and *c*) show that the model is able to capture most of the ice core and direct iron deposition stations (circles, triangles and diamonds in **Figure 1***c*, R = 0.62), but there is greater spread in the comparison when the marine sediment trap data are included (pluses in **Figure 1***c*, R = 0.42). Annual averaged concentrations from a model of iron based on 3.5% iron in mineral aerosols and combustion sources of iron (Luo et al. 2008) are shown in **Figure 2***b* and *c* compared with the available data. This demonstrates that over five orders of magnitude, model simulations can generally capture the distribution of iron in the atmosphere, with some exceptions [R = 0.78 at the long-term measuring stations (circles and triangles), R = 0.49 including cruise data]. Because dust events are episodic in nature, they tend to occur on a few days each year, and it is these few events that dominate the overall concentrations and deposition (**Figure 3** and next section). Thus, because it is unlikely that any individual observation will be taken on the few days each year that have elevated dust, the comparison of annual averaged model concentrations and daily averaged observations should result in the model values being a factor of 50–1000% higher than daily averaged observations. Accordingly, we show the individual cruise observations as a separate symbol in **Figure 2***c*, and do not always include them in the correlations. However, these results do suggest that the model overpredicts dust (and iron) in places with very low concentrations and depositions such as in the South Pacific (Wagener et al. 2008) and the eastern and western

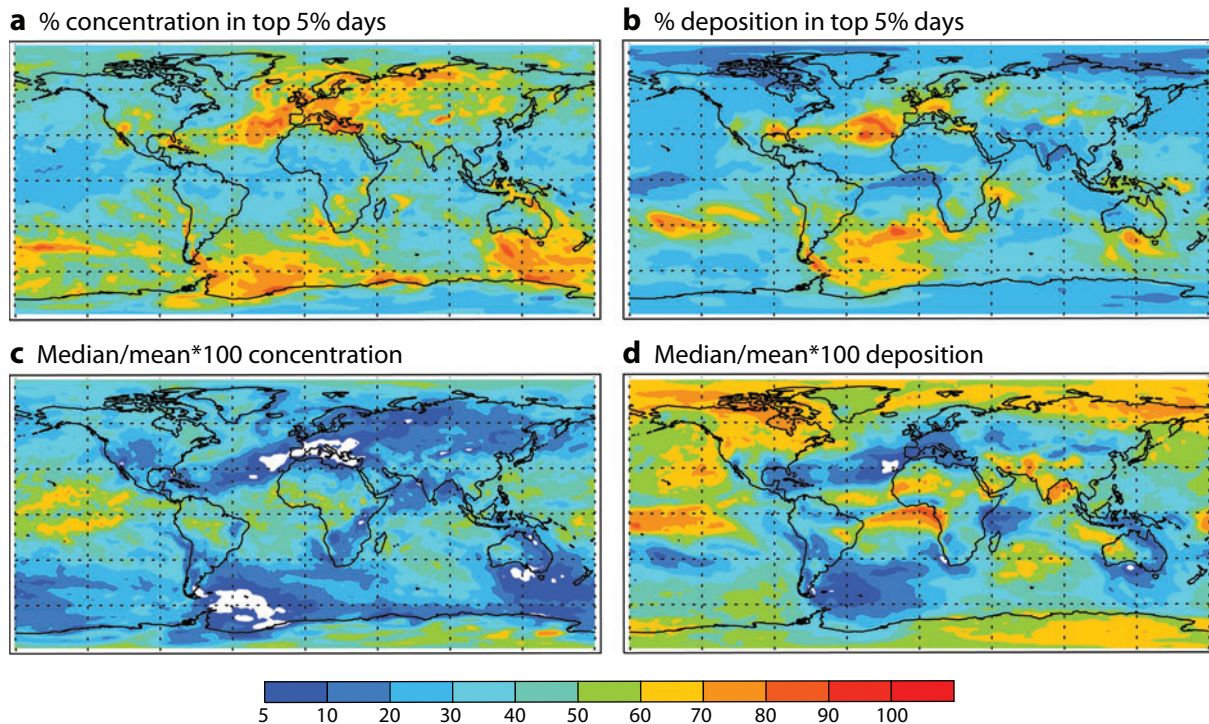←––

Figure 2

Concentration of iron in surface aerosols (μg m^{-3}) in (*a*) the observations, (*b*) a model, and (*c*) a scatter plot comparison. The location of long-term (>3 days) monitoring stations for iron are shown with an 'X'; the location of dust measurement stations are shown with a 'O' in **Figure 1***a*. For (*c*), the long-term monitoring stations for iron are shown with a filled-in circle and long-term monitoring stations for dust (and converted to iron by multiplying by 3.5%) are shown with a triangle. Individual cruise iron concentrations are shown with a '+', and individual observations where iron concentrations are inferred (from Al) are shown with a '*'. The data shown in this figure are provided in **Supplemental Table 2**, with the exception of unpublished data from L. Shank and A. Johansen.

a % concentration in top 5% days

b % deposition in top 5% days

c Median/mean*100 concentration

d Median/mean*100 deposition

5   10   20   30   40   50   60   70   80   90   100

Figure 3

Model results showing percent of dust concentration annual average in top 5% of days using model described in (*a*) Luo et al. 2003 and (*b*) for deposition. The percent of the mean, which the median represents, is shown for (*c*) concentration and (*d*) deposition from the same model.

tropical Pacific (Prospero & Bonnati 1969, Winckler et al. 2008; L. Shank & A. Johansen, personal communication).

The particle size of iron and dust aerosols is important for calculating the transport and deposition patterns, because the size of the aerosols controls the atmospheric lifetime of the aerosols to dry deposition (e.g., Tegen & Fung 1994, Foret et al. 2006). Size-segregated data exist for some of the locations shown in **Figure 2**, but generally more information on size distributions would improve our ability to constrain the transport and deposition. For example, data from Hand et al. (2004) show that the model used in **Figure 2b** has too many small particles and too few coarse particles. Including particle size information in our estimates would slightly improve our ability to simulate the long-range transport to remote ocean regions, where the model overpredicts concentrations, but this is not the only problem with the simulation. Indeed, some recent data suggest that a greater proportion of iron is contained in the large size fraction (>10 um) and is carried longer distances than previously thought (e.g., Neff et al. 2008; L. Shank & A. Johansen, personal communication).

Temporal Variability in Deposition

Because the temporal variability of iron has not been well studied, we focus in this section on the variability of the most predominant source of iron, namely the mineral aerosol. An important facet of long-range transport of pollution, especially of mineral aerosols, is that elevated concentrations occur very episodically with high temporal and spatial variability (e.g., Loye-Pilot & Martin 1986,
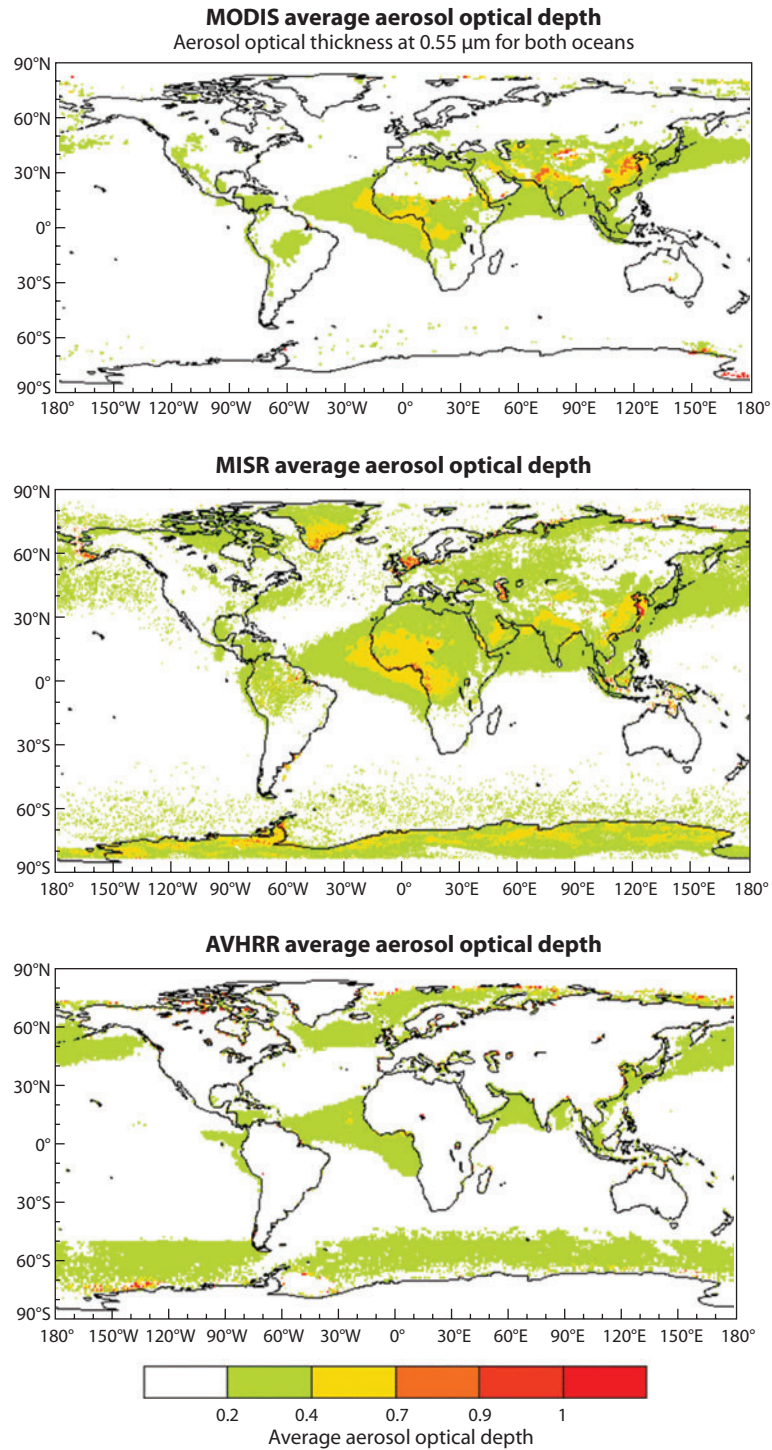
Kubilay et al. 2000, Redemann et al. 2006, Chen et al. 2007). Model results that capture this highly episodic nature of dust (e.g., Mahowald et al. 2003, Jones et al. 2003) show that 30–90% of the annually averaged dust deposition is seen on 5% of the days, those with highest deposition rates (**Figure 3a**), especially on the fringes of the dust regions. In some places, concentration is slightly less episodic than deposition, according to the model (**Figure 3b**). As an example, concentration and deposition data collected in Florida suggest that up to 90% of the deposition and most of the concentration can occur in just five days (Prospero et al. 1987), consistent with this general picture of a few large events dominating variability, especially at this location in the model (**Figure 3**). Therefore, the median represents 5–90% of the mean value in concentration, and 5–50% of the deposition (**Figure 3c** and **d**). Interpreting individual dust concentration or deposition measurements in terms of their long-term variability requires large uncertainty estimates (up to a factor of 20).
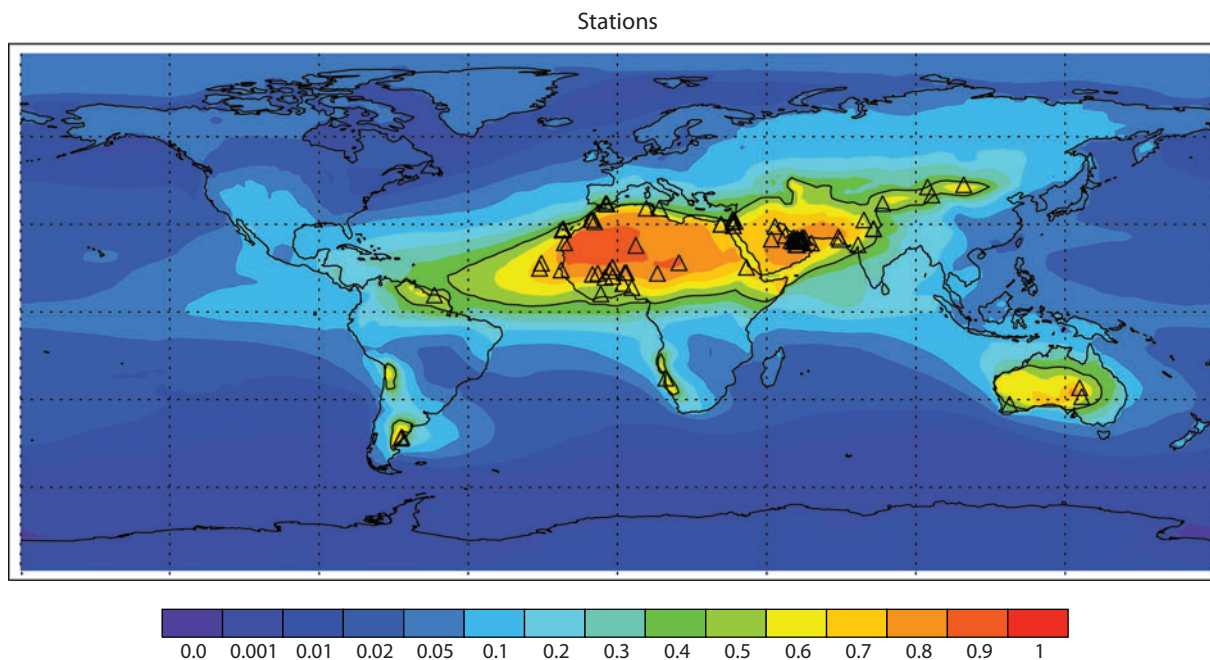
Not only do we want to know something about the global mean distribution of deposition of iron, but we often also want to know the deposition history at some particular site. There are several ways to infer this information, but this is directly measured in a very few places. Of course, long-term simulations of dust deposition using a consistent reanalysis (combination of model and observations) meteorology offer one tool for estimating interannual variability in dust and these have been evaluated against available observations (Mahowald et al. 2003). However, it is important to also include observational data in studies of temporal variability in iron deposition (e.g., Mahaffrey et al. 2003, Patra et al. 2007, Chen et al. 2007). Here we discuss the advantages and disadvantages of available datasets.

We can obtain information about deposition spatial and temporal variability from measured aerosol optical depth (AOD). AOD is a measure of the amount of direct solar radiation scattered or absorbed in the atmospheric column. Many in situ (e.g., Holben et al. 2001) and satellite measurements of AOD are available (e.g., Husar et al. 1997, Zhang & Christopher 2003, Tanré et al. 1997, Remer et al. 2005). These data provide good information about aerosol distributions for calculating the climate effect of aerosols, especially over oceans (**Figure 4**), but are more problematic when used to estimate spatial or temporal variability in iron deposition or sources. The foremost problem is that iron or mineral aerosols are not the dominant aerosol fraction in these datasets (e.g., Tegen et al. 1997), except very close to dust source regions (**Figure 5**). We show in **Figure 5** an estimate of the locations where mineral aerosols represent more than 50% of the AOD from the Rasch et al. (2001) aerosol model, which is qualitatively similar to previous estimates (Tegen et al. 1997, Cakmur et al. 2001). Other aerosols, such as sea salts over the oceans or anthropogenic aerosols near industrialized regions, are more important, and thus spatial and temporal variability in the aerosol optical depths do not represent variability in dust or iron. However, during specific dust outbreaks the plume of elevated AOD is a valuable tool for following events (e.g., Ginoux et al. 2001, Grousset et al. 2003). In addition, we need to remember that AOD variability is not identical to aerosol deposition variability, because what is seen by satellite is NOT equivalent to the aerosol deposited on the ground (e.g., Bory et al. 2002, Mahowald et al. 2003), especially because the biogeochemically relevant size fraction is much larger than the optically relevant size fraction (Dulac et al. 1992). Models are a good tool for estimating the relationship between some known quantity (e.g., satellite-derived AOD) and a desired quantity (deposition), keeping in mind that no model is perfect. In a model of dust the spatial correlation between deposition and AOD is 0.70, which means that if one knew perfectly the spatial distribution between dust AOD and deposition, we would be able to estimate 50% of the spatial variability in deposition (Mahowald et al. 2003). Similarly, the temporal variability of AOD (seasonal cycle or interannual variability) is well correlated with deposition only in certain locations (**Figure 6a** and **b**). Generally, surface concentrations are better correlated with deposition both spatially

Figure 4

Annual averaged satellite aerosol optical depths from (*a*) Moderate Resolution Imaging Spectroradiometer (MODIS) for 2000–2007 (Remer et al. 2005), (*b*) Multiangle Imaging Spectroradiometer (MISR) for 2000–2006 (Zhang & Christopher 2003), and (*c*) Advanced Very High Resolution Radiometer (AVHRR) for 1982–June 2006 (Husar et al. 1997). Aerosol optical depths were downloaded from **http://ladsweb. nascom.nasa.gov/ data/search.html**, **http://eosweb.larc. nasa.gov/**, and **http://gacp.giss.nasa. gov/data_sets/**.

MODIS average aerosol optical depth

Aerosol optical thickness at 0.55 μm for both oceans

MISR average aerosol optical depth

AVHRR average aerosol optical depth
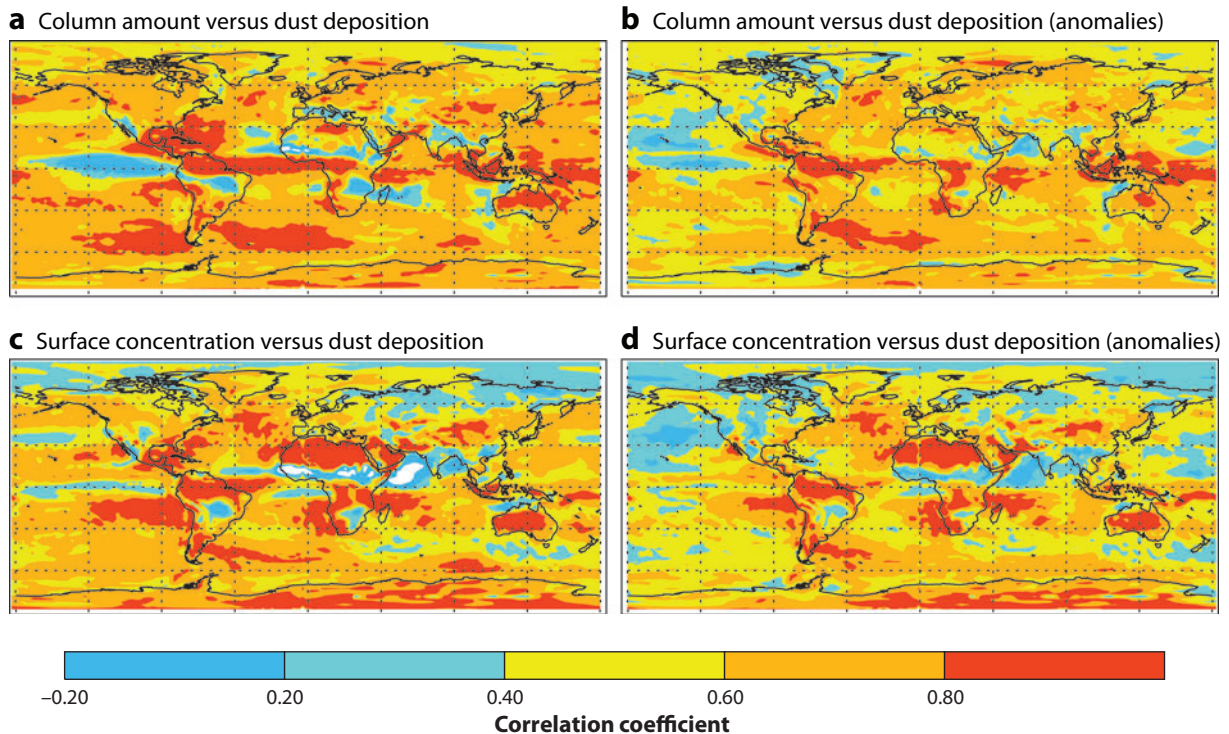
Average aerosol optical depth

Figure 5

Fraction of aerosol optical depth from desert dust, as estimated from a model (Rasch et al. 2001), and the location of Aerosol Robotic Network (AERONET) sites in dust-dominated regions (*triangles*) (Holben et al. 2001) (**http://aeronet.gsfc.nasa.gov/**).

(R = 0.86) and temporally (Mahowald et al. 2003) (**Figure 6c** and **d**). But in some locations deposition is temporally anticorrelated with both surface concentration and AOD (**Figure 6**). In addition to satellite data, high-quality surface measurements of AOD are available from Aerosol Robotic Network (AERONET) sites, many of which are located in dust-dominated regions (Holben et al. 2001) (**http://aeronet.gsfc.nasa.gov/**). AERONET-derived measurements provide information about AOD in a high temporal resolution that in some cases extends back into the 1990s. These data have been very useful in improving models and our understanding of dust (e.g., Ginoux et al. 2001, Luo et al. 2003, Balkanski et al. 2007).

As stated above, often higher temporal correlations exist in the model between surface concentrations and deposition. This finding implies that using the high-quality concentration data when available is also a good option for understanding temporal variability in deposition (highlighted in **Figure 1**). Concentration data can represent interannual variability in dust deposition on a regional scale in some cases (see Mahowald et al. 2003 for specific estimates); although expensive to acquire, these datasets represent our best quality datasets for understanding variability in specific species.

One can also look in the source regions to understand variability in dustiness and infer the impacts on the variability in depositions. To do this, one must estimate the aerial extent impacted by a particular dust source. There are several apportionment studies available from models (Luo et al. 2003, Tanaka & Chiba 2006, Mahowald 2007): Only Mahowald (2007) focuses on contribution to deposition, as opposed to column amount (**Figure 7**). The model is able to generally capture the geochemical provenance data (e.g., see Grousset & Biscaye 2005 for review), with the important exception of Greenland, where the models (Luo et al. 2003, Tanaka & Chiba 2006) predict a
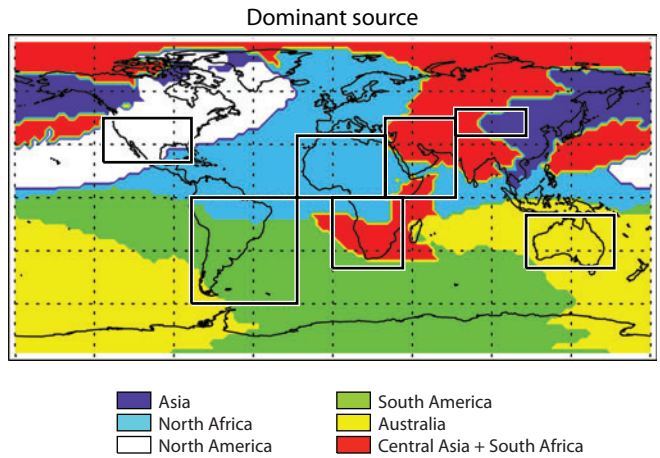
a Column amount versus dust deposition

b Column amount versus dust deposition (anomalies)

c Surface concentration versus dust deposition

d Surface concentration versus dust deposition (anomalies)

| –0.20 | 0.20 | 0.40 | 0.60 | 0.80 |

Correlation coefficient

Figure 6

(*a*) Correlation coefficient of monthly mean modeled dust deposition and column amount at a given gridpoint over the time period 1979–2003 (Mahowald et al. 2003). (*b*) Correlation coefficient of the monthly anomalies in dust deposition and column amount (seasonal cycle is removed). (*c* and *d*) Correlation coefficients for the surface concentration.

dominance of North African dust, whereas the geochemical data suggest the dominance of Asian dust (e.g., Bory et al. 2003).

For looking in the dust source areas, the Total Ozone Mapping Spectrometer (TOMS) absorbing aerosol index (AAI) (Herman et al. 1997) is often used because it is able to retrieve an aerosol index over land (Torres et al. 1998, Prospero et al. 2002). **Figure 8** shows the distribution of dust source hotspots on the basis of the TOMS AAI, whereby hotspots are associated with local maxima in the long-term mean TOMS AAI (1984–1990) (Engelstaedter & Washington 2007). The TOMS AAI is most stable over the time period 1984–1990 (see TOMS web page at **http://aeronet.gsfc.nasa.gov/**). The TOMS AOD uses a combination of model output and TOMS AAI to infer an AOD (Torres et al. 2002), but in some dust regions problems exist with the seasonal cycle and variability derived using this tool (e.g., Bryant et al. 2007, Mahowald et al. 2007).

Another dataset, based on meteorological station data (collected at airports globally) shows a different distribution of dustiness (Engelstaedter et al. 2003, Mahowald et al. 2007) (**Figure 9**). Several different estimates of dustiness can be obtained from these records, and the ones that are best able to capture the variability in AOD seen at nearby AERONET stations are the fraction of visibility events (<5km) and the extinction (a function of 1/visibility) (Mahowald et al. 2007). These data are also available for 1974–2003, and thus represent a relatively long time record of dustiness in the source regions.

Dominant source

|	Asia		South America
	North Africa		Australia
	North America		Central Asia + South Africa

Figure 7

Source apportionment study from Mahowald (2007) based on model used in Mahowald et al. (2006). Colors show which regions dominate the deposition at a given grid box.

Decadal Variability in Dust

Long time series of in situ concentration measurements at Barbados (Prospero & Nees 1986, Prospero & Lamb 2003) have shown a fourfold increase in dustiness between the 1960s and the 1980s. This variability in dust is correlated with a decrease in the Sahel precipitation, and the correlation bcomes slightly higher if the previous year's precipitation is considered (Prospero & Lamb 2003). Barbados is downwind from the North African source, and so these changes can
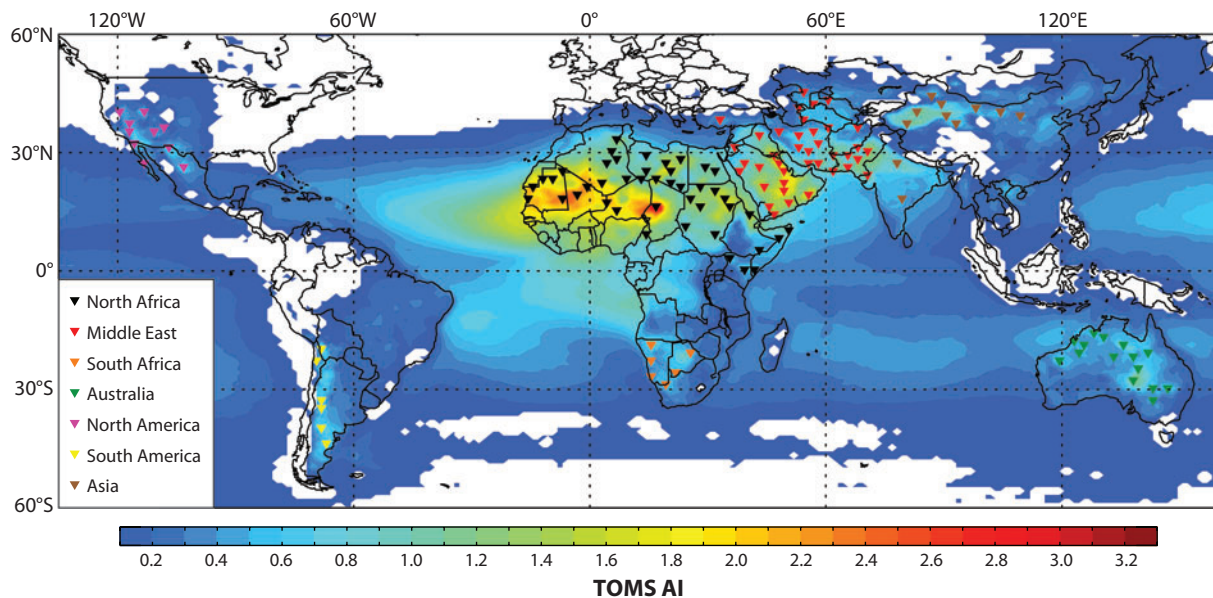
Figure 8

Long-term mean Total Ozone Mapping Spectrometer absorbing aerosol index (TOMS AAI) (Torres et al. 2002) averaged between 1984 and 1990 and dust source hotspots as identified in Engelstaedter & Washington (2007) (*triangles*).

Figure 9

Averaged visibility derived dustiness indicators for desert dust regions for (*a*) fraction of visibility events less than 5 km, (*b*) extinction, (*c*) fraction of visibility events less than 1 km and (*d*) blowing dust or sand. Taken from Mahowald et al. (2007) and Engelstaedter et al. (2003) with permission of authors.

a VIS5

Fraction of time

b EXT

Aerosol optical depth (fraction)

c VIS1

Fraction of time

d Blowing dust or sand

Fraction of time
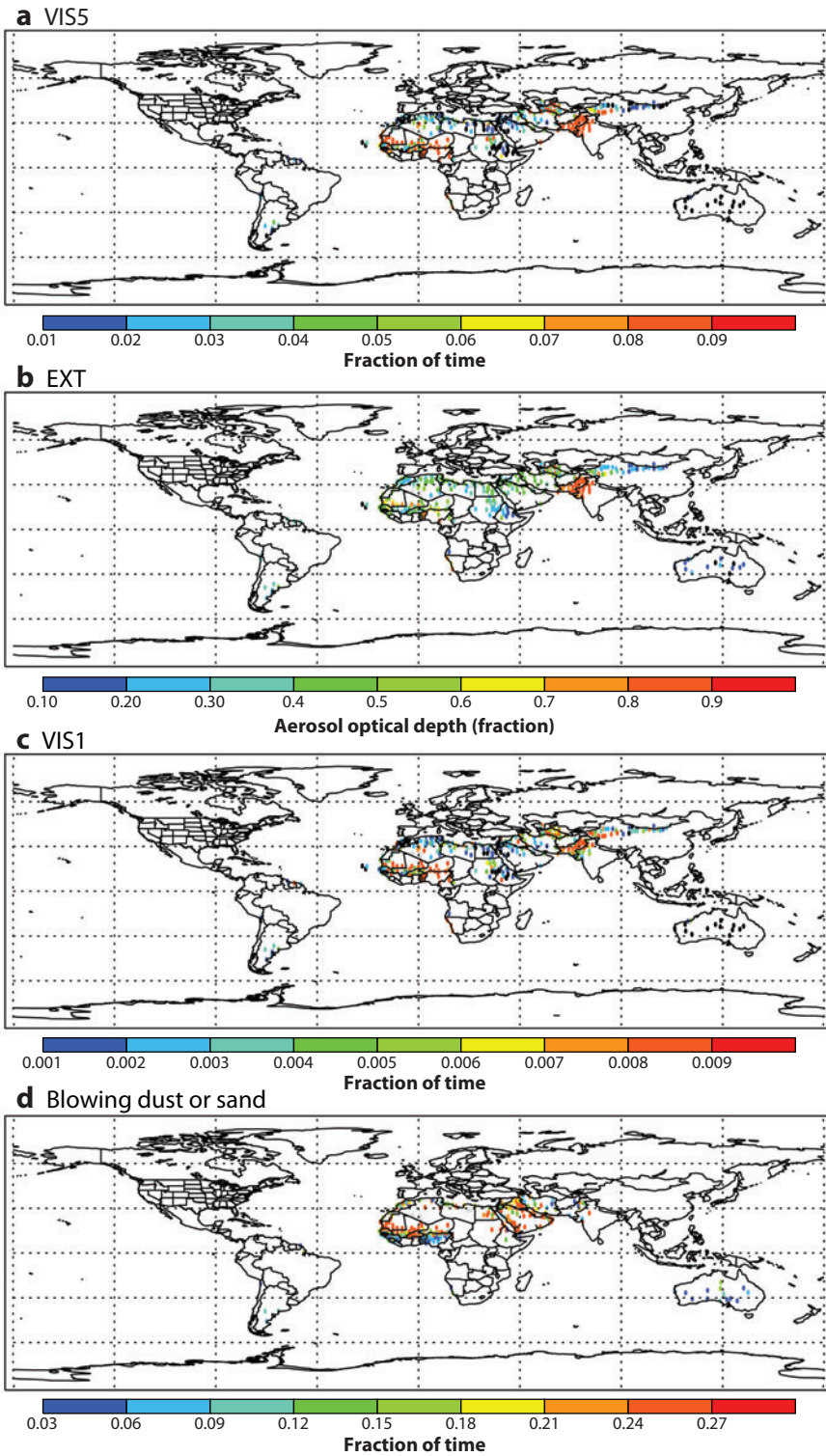
represent changes in source strength and/or changes in transport efficiency. Analyses of visibility data in North Africa show similarly large changes in dustiness in the source regions (Mbourou et al. 1997, Mahowald et al. 2007), suggesting that much of this dust variability derives from the dust source.

Despite high interannual variability, change in deposition in the northwestern Mediterranean Sea was on average an increase by a factor of 3–4 from the mid-1980s to the mid-1990s (Ridame et al. 1999), although aerosol optical depths show a different signal (Moulin et al., 1997b). This change in dust is likely to be strongly driven by the changes in precipitation, because wetter soils will inhibit dust emissions, as well as remove atmospheric dust. Humans may also play a role in modulating these changes. Precipitation changes in the Sahel are likely related to sea surface temperature changes in the North Atlantic and/or the Indian ocean (e.g., Giannini et al. 2003, Hoerling et al. 2006), some of which may be associated with global warming (Giannini et al. 2003). Anthropogenic aerosols from industry may also be contributing to the drought (Rostayn & Lohman 2002). The role of human degradation of the land surface may also be important (e.g., Charney et al. 1977, Xue & Shukla 1993). Dust may be responsible for up to 30% of the decrease in precipitation over the Sahel (Yoshioka et al. 2007). As discussed below, humans may have perturbed dust significantly in North Africa (e.g., Moulin & Chiapello 2006, Yoshioka et al. 2007), so this direct perturbation of dust could be contributing to the change observed at Barbados (Mahowald et al. 2002). The poorly known change in human land use in the Sahel may have occurred at a similar rate as the observed change in dust (Mahowald et al. 2002). In recent years, the Sahel drought has recovered to close to average values, but the dust in Barbados has not (Prospero 2006), and the correlation between dust and precipitation no longer holds, suggesting more complicated mechanisms may be involved (**Figure 10**).

Some studies have identified the correlation of climate indices with dust distributions (Moulin et al. 1997a, Mahowald et al. 2003). **Figure 11** shows an estimate of modeled dust correlations with El Nino and the North Atlantic Oscillation (NAO) over the time period 1979–2006 (updated from Mahowald et al. 2003). This model's ability to capture interannual variability has been shown to be good (Mahowald et al. 2003), which suggests that large regions of the oceans will
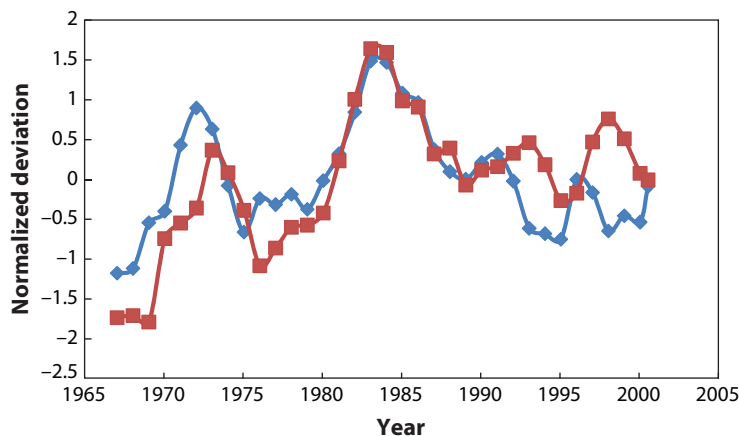
Figure 10

Time series of dust at Barbados (Prospero & Nees 1986, Prospero & Lamb 2003) (*red line*) and the negative of the Sahel precipitation anomaly (Chen et al. 2002) (*blue line*), both normalized by removing the mean and dividing by the standard deviation.

a Deposition correlated with El Nino 3.4

b Deposition correlated with NAO

0.20	0.4	0.6	0.8

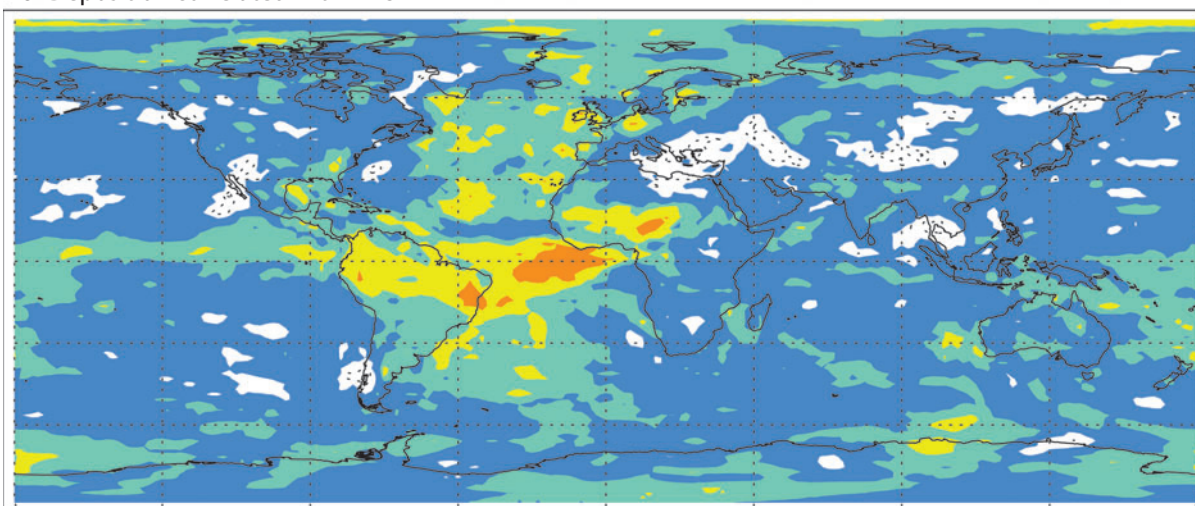**Correlation coefficient**
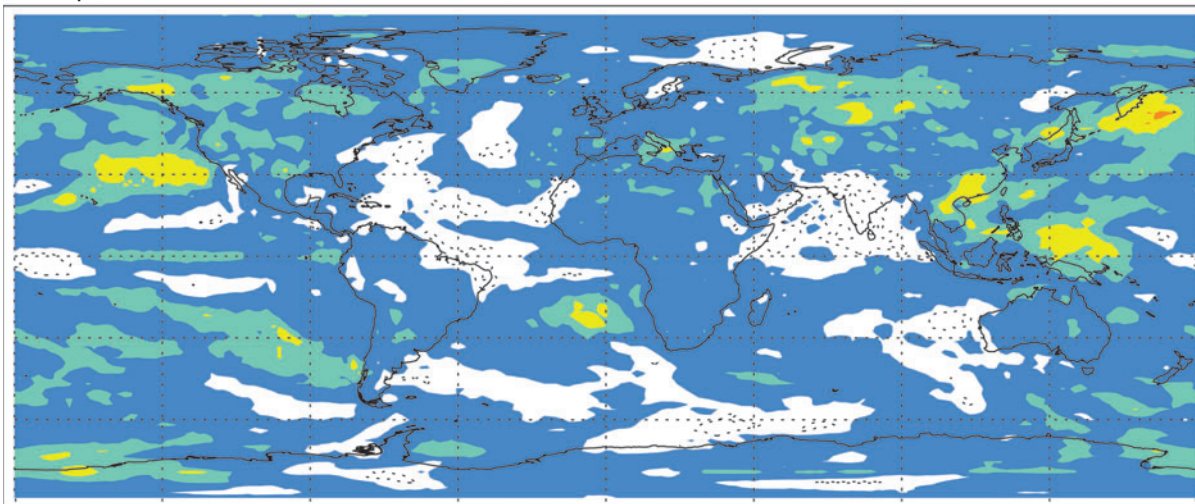
Figure 11

Correlation of modeled deposition (1979–2006 from Mahowald et al. 2003) with El Nino (**http://www.cpc.ncep.noaa.gov/products/ analysis_monitoring/ensostuff/ensoyears.shtml**) and North Atlantic Oscillation (**http://www.cgd.ucar.edu/cas/jhurrell/indices. html**) (Hurrell et al. 2001).

experience similarly high or low deposition during El Nino and NAO periods. This synchronicity in the changes could have important consequences for ocean biogeochemistry. There are no data showing El Nino dust relationships, perhaps because of the sparse longer time series in the impacted region (see Mahowald et al. 2003 for more discussion).

BIOAVAILABLE IRON

The bioavailable fraction of iron deposited onto the ocean's surface is not well known, but it is often assumed to be the fraction of iron in Fe(II) or the labile iron fraction (e.g., Zhu et al. 1997, Jickells & Spokes 2001, Mahowald et al. 2005), although Fe(III) may also be bioavailable (Barbeau et al. 2001) and Fe(II) is not always bioavailable (Visser et al. 2003). Some researchers have argued that almost all incoming iron may be bioavailable, depending on the timescale and biological community (e.g., Weber et al. 2005). This lack of understanding is confounded by the speciation and complexation of oceanic iron by poorly characterized ligands (Parekh et al. 2004; Bergquist et al. 2007; T. Wagener, E. Pulido-Villena, C. Guieu, submitted manuscript). Both Fe(II) and labile iron are measured by some groups, and a compilation of data from several cruises is shown in **Figure 12** (and in **Supplemental Table 2**). Notice that compared with total iron, substantially less data shows the distribution of soluble iron.
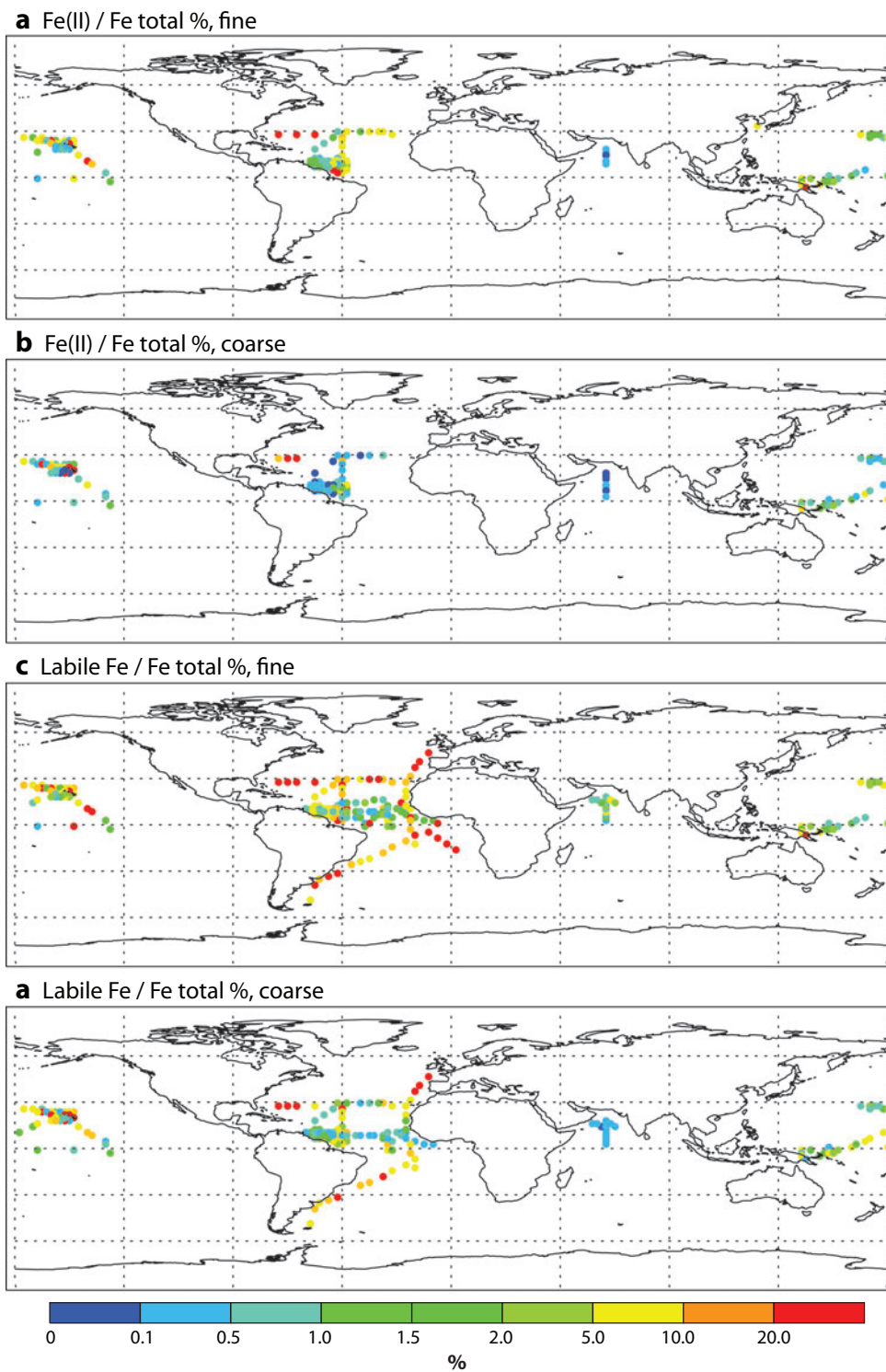
Soluble iron deposition has been measured in a few studies. Iron in rainwater has solubilities ranging from 4% to 50% (reviewed by Jickells & Spokes 2001, Kieber et al. 2001, Ozsoy & Saydam 2001, Kieber et al. 2003). Edwards & Sedwick (2001) measured a mean of 30% solubility of iron in and near Antarctica in snow and ice, whereas R. Losno & F. Dulac (personal communication) measured refractory iron at 30%–70% solubility in aerosol deposition at Kergulen Island (49 S, 70 E) after two years of soaking in acid at pH 1. Relatively high solubilities were measured in the equatorial Pacific, another remote region (L. Shank & A. Johansen, personal communication) (**Figure 12**). More measurements and consistent measurement techniques would assist in the assessment of iron solubility (e.g., Zhu et al. 1997, Mackie et al. 2005, Chen et al. 2006).

The source of soluble iron remains enigmatic. Several studies suggest that most of the soluble iron is derived from processing in the atmosphere (e.g., Jickells & Spokes 2001, Mahowald et al. 2005), because soils have relatively low iron solubilities ($\sim$0.1%) (Fung et al. 2000, Hand et al. 2004), whereas atmospheric iron has solubilities ranging from 0.01% to 80% (e.g., Siefert et al. 1999, Johansen et al. 2000, Baker et al. 2006a, Baker et al. 2006b) (**Figure 12** and **Supplemental Table 2**). This solubilization may be due to atmospheric acids (see Mahowald et al. 2005 for a review) such as sulfate and organic acids. Several studies have linked the natural sulfur and iron cycles, which might allow ocean biota to regulate the bioavailability of incoming iron (Johansen & Key 2006, Zhuang et al. 1992). Meskhidze et al. (2003 and 2005) suggested a specific mechanism in the atmosphere for converting hematite iron to become more soluble in the presence of strong acid. Modeling of the atmospheric processing of iron showed that because of the limited observations, many different mechanisms are equally likely to match available observations (Hand et al. 2004, Luo et al. 2005, Fan et al. 2006).

However, more recent data have suggested that combustion sources of soluble iron may be important (Guieu et al. 2005, Chuang et al. 2005, Sedwick et al. 2007). Evidence suggests that combustion sources of iron have a high bioavailability, estimated to be between 2% and 19% (using inconsistent measures of bioavailability) (Bonnet & Guieu 2004, Guieu et al. 2005, Chuang et al. 2005, Sedwick et al. 2007). In contrast, aerosols from desert regions are thought to be approximately 0.4% soluble (Chuang et al. 2005, Chen et al. 2006, Sedwick et al. 2007). Subsequently, a modeling study suggested that the best match to available data included substantially higher solubilities of iron in combustion aerosols than in dust (4% versus 0.4%) (Luo et al. 2008). Because combustion particles tend to be smaller, they have a longer lifetime, and would explain the higher solubilities farther downwind (Luo et al. 2008). Indeed, some studies suggest no apparent change in the solubility of iron particles as they move downwind from the North African source, although there is a change in the phosphorus solubility in the same samples (Baker et al. 2006b). Most of the data suggests smaller particles have higher solubilities (e.g., Siefert et al. 1999, Baker

Observed aerosol solubility of iron using (*a*) Fe(II) as soluble and (*b*) labile iron as soluble. Observations are compiled in **Supplemental Table 2**, with the exception of equatorial Pacific data, which is courtesy of L. Shank and A. Johansen.

a Fe(II) / Fe total %, fine

b Fe(II) / Fe total %, coarse

c Labile Fe / Fe total %, fine

a Labile Fe / Fe total %, coarse

0   0.1   0.5   1.0   1.5   2.0   5.0   10.0   20.0

%

& Jickells 2006), which is consistent with smaller particles having a longer lifetime and thus experiencing more atmospheric processing (Hand et al. 2004) and larger surface area per mass, or with a combustion source of soluble iron (Luo et al. 2008). Journet et al. (2008) shows that the most bioavailable fraction of iron in dust is not the iron oxides (e.g., hematite), which have a high fraction of iron (50–80%), but rather the clay component, which accounts for more than 90% of the soluble iron. Because many of the existing models of atmospheric processing focus on the iron solubility of hematite (Meskhidze et al. 2003, Meskhidze et al. 2005, Luo et al. 2005, Fan et al. 2006), this result requires us to revisit the issue of iron processing by acids in the atmosphere. Much of this atmospheric processing of iron would occur in clouds or at least in regions with high specific and relative humidity, consistent with relatively high solubilities of iron in precipitation (e.g., Saydam & Senyuva 2002).

As an example, we show modeled soluble iron deposition from three different scenarios, taken from Luo et al. (2008), in **Figure 13**: Scenario I is only atmospheric processing, Scenario II is only direct emissions of soluble iron (combustion iron is soluble at 4%, whereas dust iron is soluble at 0.4%), and Scenario III combines Scenario I and II. The latter two scenarios are equally consistent with available observational data (shown in Luo et al. 2008), whereas Scenario I (atmospheric processing only) cannot match observations at Cheju (Chuang et al. 2005, Luo et al. 2008). The scenarios that match the available data show increasing solubility of aerosols as they move farther from the source regions. **Table 1** shows an estimate of the iron and soluble iron inputs to various oceans based on this model simulation (total iron inputs for various model and observational estimates are reviewed in Mahowald et al. 2005). In the current climate, the North Atlantic receives more total iron inputs, whereas the North Pacific receives more soluble iron according to these estimates because of changing emissions (based on Scenario III, both atmospheric processing and emissions). This is consistent with ocean iron observations that suggest similar concentrations in the Pacific and Atlantic (Boyle et al. 2005). Notice that these model results suggest that estimates of high nitrogen fixation rates in the Pacific are still consistent with high atmospheric soluble iron inputs, in contrast to the arguments of Deutsch et al. (2007).
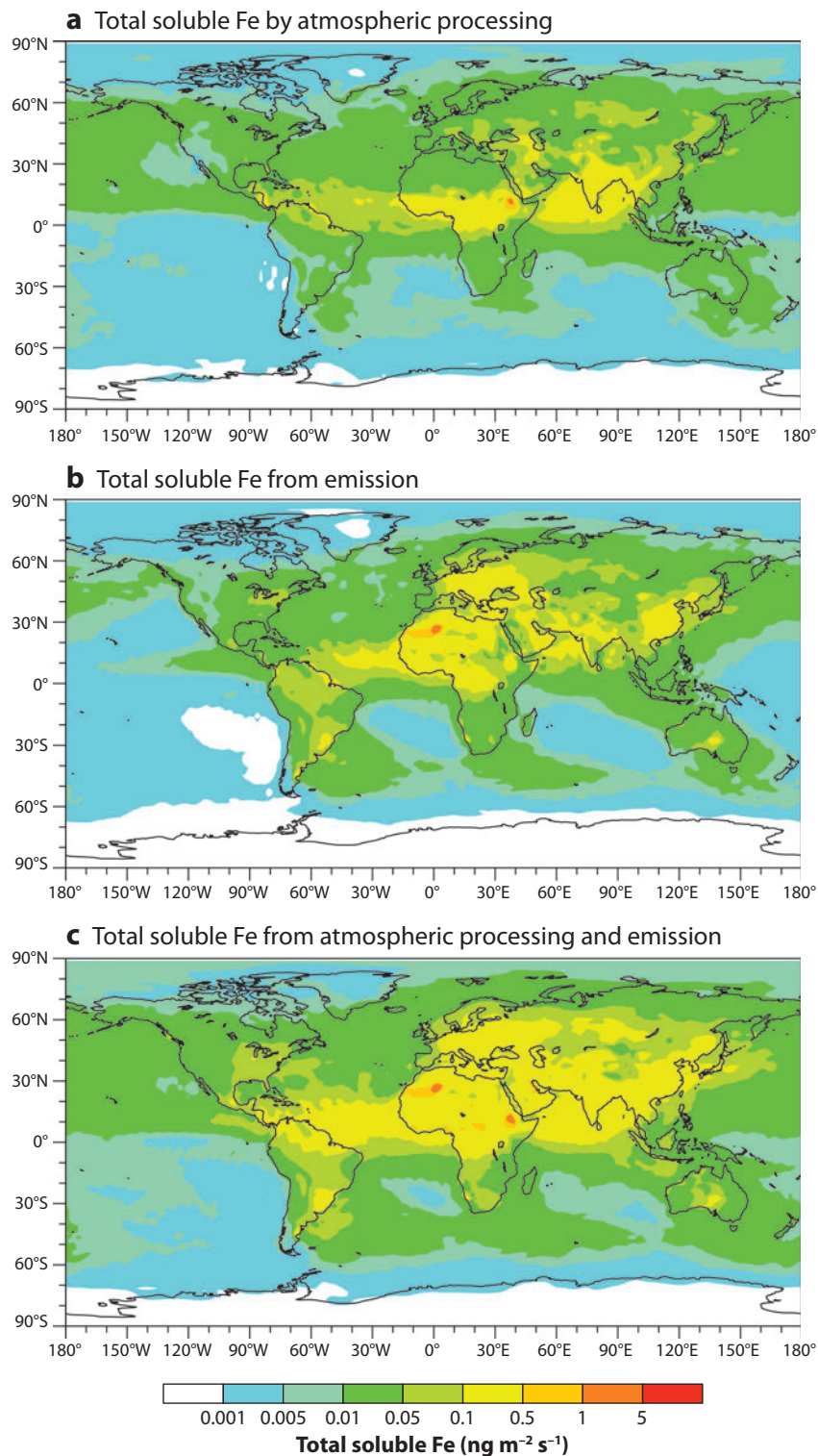
HUMAN PERTURBATIONS TO DUST

There are many ways in which human activities can impact mineral aerosol entrainment into the atmosphere. Because mineral aerosols dominate the atmospheric iron budget, any changes in mineral aerosols budgets will be important. Human land use changes such as agriculture or pasturage remove the vegetative cover and perturb soil layers, making regions better sources of dust (e.g., Gillette 1988, Neff et al. 2005). Water use can convert lakes to dry lake beds, which then become additional sources for wind erosion [e.g., dry Lake Owens in California (Gill 1996, Cahill et al. 1996)]. In addition, human-induced climate change can alter precipitation patterns, which may affect the occurrence of drought conditions in many regions (Dai et al. 2004). Conversely, increases in carbon dioxide can make arid species more able to deal with water stress and increase the productivity of plants (Smith et al. 2000). Here we discuss the state of research on human impacts on atmospheric desert dust emissions.

The importance of human land use to the modification of dust sources is not well understood. Some studies have argued that the majority of dust sources are natural topographic lows, based on analysis of the TOMS AAI (mean TOMS AAI shown in **Figure 8**) (Washington et al. 2003, Prospero et al. 2002). However, this dataset is biased toward the identification of sources with the highest vertical mixing, which tends to be during summer and in the center of desert regions (Mahowald & Dufresne 2004). Furthermore, the TOMS AAI may be misleading in some regions as a result of a bias due to its sampling time of one measurement per day at approximately noon

Model predictions of
soluble iron deposition
using (*a*) Scenario I
(atmospheric
processing),
(*b*) Scenario II (direct
emissions of soluble
iron), and (*c*) Scenario
III (combination of
Scenarios I and II).
From Luo et al. (2008).

a Total soluble Fe by atmospheric processing

b Total soluble Fe from emission

c Total soluble Fe from atmospheric processing and emission

0.001 0.005 0.01 0.05 0.1 0.5 1 5

Total soluble Fe (ng m⁻² s⁻¹)

Table 1   Budgets for different ocean basins (Tg/yr) based on simulations described in Luo et al. (2008) for Scenario III

	Total Fe	Soluble Fe (current)	Soluble Fe (preindustral)
North Pacific	0.96	0.046	0.019
South Pacific	0.51	0.015	0.0076
North Atlantic	6.38	0.067	0.043
South Atlantic	0.68	0.020	0.0086
South Indian Ocean	0.21	0.013	0.0050
North Indian Ocean	1.99	0.046	0.013
Antarctic	0.0031	9.35e-5	6.82e-5
Arctic	0.017	0.00067	0.00029
Mediterranean Sea	0.017	0.00015	9.37e-5

local time (orbiting satellite), and the multiple detection of locally stationary elevated dust (may stay elevated for up to three days in the same region), which may be misinterpreted as an active dust source (Schepanski et al. 2007). Other analyses of the TOMS AAI argue for large sources of anthropogenic dust from North Africa (Yoshioka et al. 2005, Moulin & Chiapello 2006).

Part of the problem is that dust source characteristics and the processes that control emissions are not well understood. For instance, dust sources may be associated with the occurrence of surface features such as lake and fluvial deposits, dunes, or anthropogenically disturbed soils, which may act as sources for dust emission or may support dust generation and entrainment into the atmosphere (e.g., Warren et al. 2007). **Figure 14** shows an analysis of the dust hotspots from Engelstaedter & Washington (2007) (from **Figure 8**), whereby the hotspots are classified according to the occurrence of four surface characteristics identified from cartographic material (Times Atlas of the World, 1999) and satellite imagery (Google Earth). Although this qualitative approach may be subject to errors due to poor quality of the source material and the poor ability to resolve sources, it shows that for the entire globe almost half (47%) of the 131 dust hotspots are associated with agriculture (**Figure 14*a***). This result does not mean that 47% of the atmospheric dust is the result of agricultural activities. The number of occurrences for salt/lake deposits (48%), fluvial deposits (62%), and dunes (45%) is of similar magnitude, indicating the occurrence of multiple surface features at many hotspots. The occurrence of multiple surface features in a source region may not be seen as a coincidence. For instance, in arid environments, agriculture is often found close to impermanent or dry rivers and lakes owing to the availability of close (ground) water and fertile soils. In these cases, quantifying the relative importance of each surface feature for dust emission is difficult. Although average TOMS AAI values associated with agriculture for the whole world are lower than for fluvial deposits and dunes (similar to salt/lake deposits), anthropogenically disturbed soils may play an important role on regional scales where values can be relatively high (e.g., Australia, North and South America and Asia) (**Figure 14**). The high number of salt/lake and fluvial deposit-associated hotspots is in good agreement with previous studies that identified topographic lows as preferential source regions (e.g., Prospero et al. 2002), whereas dunes may have a more important role than previously thought (**Figure 14**). Modeling studies have highlighted the similarity in the distribution of dust from topographic lows and cultivation in arid regions (Mahowald et al. 2002, Luo et al. 2003), which is why the dust distributions shown in **Figure 1** and **2** do not include a land use source of dust.

Other datasets have also been used to isolate the impacts of human land use. There are two types of data in meteorological station records, frequency of dust storms or blowing dust
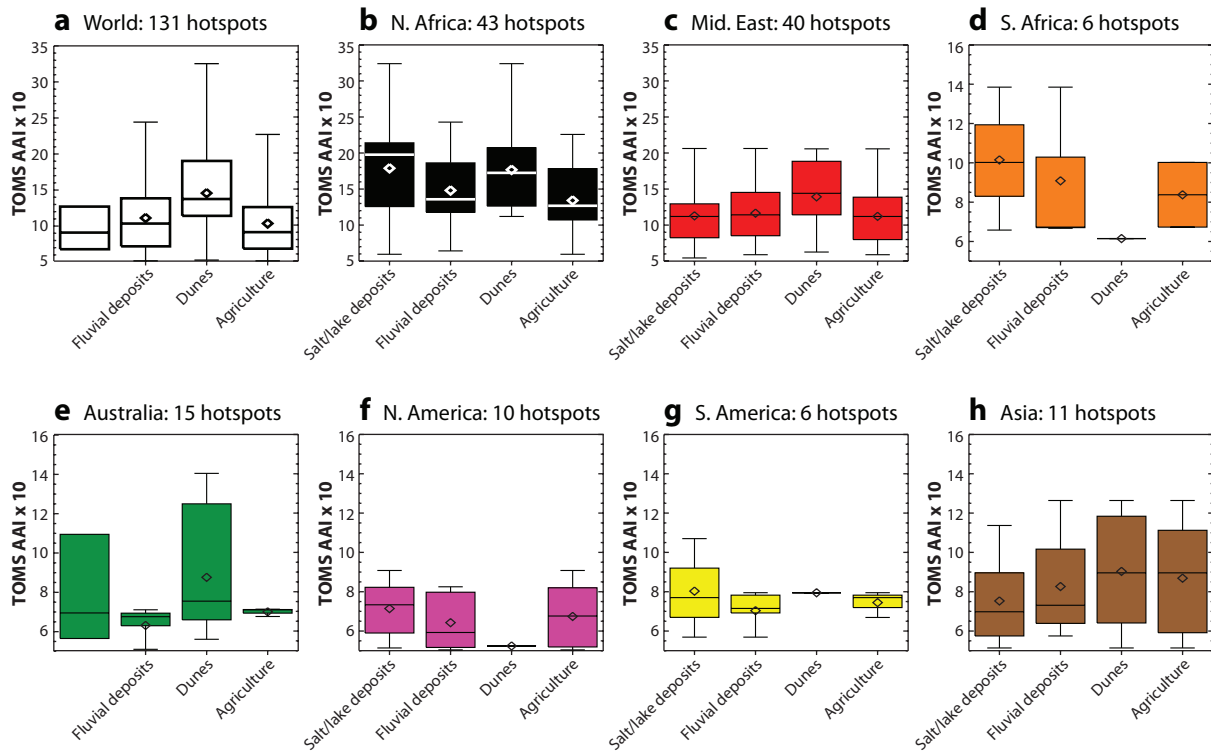
Figure 14

Variability of long-term mean Total Ozone Mapping Spectrometer absorbing aerosol index (TOMS AAI) values (1984–1990) derived from dust source hotspots as shown in **Figure 8** (Engelstaedter et al. 2003), classified by the occurrence of surface features for (*a*) the whole world and (*b–h*) specific geographic regions. Shown are the arithmetic mean (*diamond*), the median (*horizontal line through the box*), the 25th percentile (*lower edge of the box*), and the 75th percentile (*upper edge of the box*); the horizontal lines below and above the box represent the minimum and maximum value. The percentage of the number of hotspot occurrences is given above each box. Box fill colors correspond to hotspot symbol colors in **Figure 8**. Note that two different y-axis scales are used for plots *a–c* and *d–h*.

(Engelstaedter et al. 2003) and measures of visibility (Mbourou et al. 1997, Mahowald et al. 2007). Using blowing dust datasets, different models, and slightly different methodologies, Tegen et al. (2004) constrains the dust from agriculture to less than 10%, whereas Mahowald et al. (2004) shows that the dataset is consistent with between 0% and 50% agricultural dust. Thus, large uncertainties remain in the strength of the human land use source in the current climate. Regional studies are required to better constrain these numbers (Xuan & Sokolik 2002, Yoshioka et al. 2005, Moulin & Chiapello 2006), although these studies also have uncertainties associated with their methodology.

The impact of water use on the global dust cycle has not been evaluated systematically. Although local studies show the importance of water use on the dry Lake Owens (e.g., Gill 1996, Cahill et al. 1996), this source is not thought to be important globally (e.g., Prospero et al. 2002). The Aral Sea has undergone a substantial reduction in area over the past 50 years (Micklin, 1988), but there is no observed trend in dustiness in the region (Mahowald et al. 2007).

The impact of climate and increases in carbon dioxide as we move into the future have been examined (Mahowald & Luo 2003, Tegen et al. 2004, Woodward et al. 2005, Mahowald et al. 2006), but only two studies have investigated preindustrial versus current climate (Mahowald

& Luo 2003, Mahowald et al. 2006). These modeling studies predict relative small changes (+/–20%) (Tegen et al. 2004) to large decreases (–20% to –60%) (Mahowald & Luo 2003) to very large increases (+200%) (Woodward et al. 2005); in the latter the Amazon dries up in a coupled-carbon cycle study. Mahowald (2007) focused on the Intergovernmental Panel on Climate Change (IPCC) model simulations and conducted simulations of desert area changes using simulations from 17 models. In the mean the models predict an approximately 10% increase in desert area with time (from 1880s to 2100) due to increased aridity, but if carbon dioxide fertilization is included, the mean of the models predicts an approximately 4% decrease in desert area (Mahowald 2007). However, individual models predicted increases and decreases of up to 50% in desert area, suggesting large uncertainties in our predictions (Mahowald 2007). Mahowald (2007) also tried to identify desert regions that were likely to be most sensitive to climate change, but unfortunately the models do not agree on where changes in precipitation will occur.

Observational evidence of changes in atmospheric dust between the preindustrial and current climate have been difficult to use to determine trends, because most of these data are collected at long distances from the dust sources and are not regionally consistent (Mahowald & Luo 2003). Recent studies provide tantalizing new evidence for large increases in dust since preindustrial times. McConnell et al. (2007) show a doubling of dust over the twentieth century based on ice core data from Antarctica, which they attribute to changes in South American dust. Neff et al. (2008) show dust levels recorded in a lake sediment in the southwestern United States to be elevated 500% during the nineteenth century, which they attribute to increased settlement during that time period. **Figure 15** shows a compilation of current to preindustrial ratios of dust deposition from available ice and lake core records, but there are too few measurements to draw general conclusions (Donarummo et al. 2002; Mayewski et al. 1995; McConnell et al. 2007; Mosley-Thompson et al. 1990; Neff et al. 2008; Thompson et al. 1984, 1995, 2002; Zdanowicz et al. 1998, Zielinski & Mershon 1997).

Unfortunately, the relative importances of the different processes are not well known, and thus we do not know if humans have increased dust by 60% or reduced dust by 25% since preindustrial times (Mahowald & Luo 2003, Mahowald 2007).

HUMAN PERTURBATIONS TO IRON

Humans can also disturb both direct emissions of iron (through combustion sources primarily) and the bioavailability of iron by increasing the amount of acids in the atmosphere. As discussed above, evidence suggests that combustion sources of iron have a higher bioavailability and thus although iron from combustion is not important globally (<5%) combustion sources of soluble iron could represent 50% of the global iron budget (Luo et al. 2008). Additionally, humans have drastically increased sulfur dioxide emissions over the past 100 years, increasing the acidity of atmospheric aerosols (Smith et al. 2004).

Studies of atmospheric soluble iron have shown that many different hypotheses about the sources of atmospheric iron are equally consistent with available distributions of observations, largely because of the lack of data (Hand et al. 2004; Luo et al. 2005, 2008; Fan et al. 2006), as discussed above. However, the more recent data that show higher solubility of combustion iron than dust iron suggest that the combustion source of soluble iron should be included in any study (Guieu et al. 2005, Chuang et al. 2005, Sedwick et al. 2007). **Figure 16** shows the ratio of estimates of current to preindustrial deposition for the three scenarios for soluble iron production, taken from Luo et al. (2008) and shown also in **Figure 13**. Again, Scenario I is only atmospheric processing, Scenario II is only direct emissions of soluble iron (with combustion iron soluble at 4%, whereas dust iron is soluble at 0.4%) and Scenario III combines Scenario I and II. The latter two
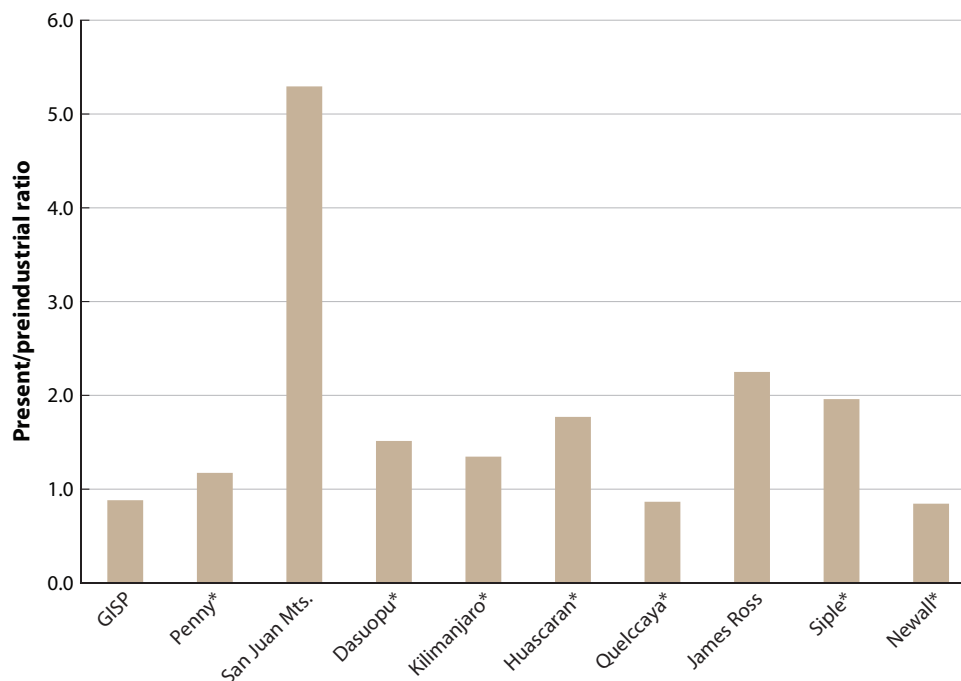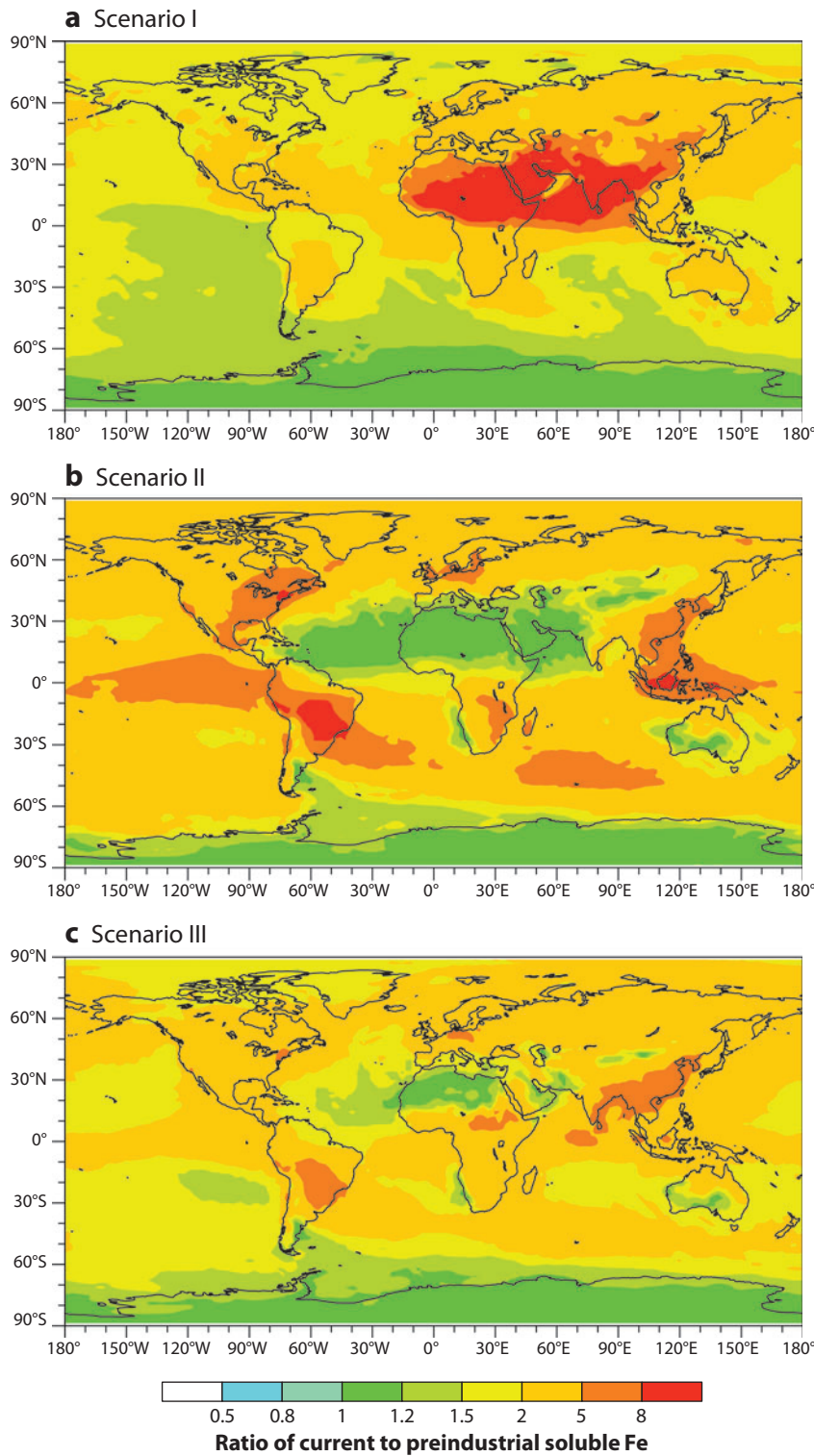
Figure 15

Current preindustrial dust ratios derived from ice core and lake sediment records. Ice core data represent mass or number concentrations (indicated by an asterisk). San Juan lake dust records are derived from Ca accumulation rates in lake sediments, and ratios here represent 1980–present/3000 BC–1850 (Neff et al. 2008). The James Ross Island dust record is derived from aluminosilicate dust fluxes; the ratio here represents 1960–1991/1832–1900 (McConnell et al. 2007). Locations of the ice and sediment cores sorted according to their latitudinal position from North to South are as follows: GISP (72°N, 38°W) (Donarummo et al. 2002, Zielinski & Mershon 1997), Penny Ice Cap (67°N, 66°W) (Zdanowicz et al. 1998), San Juan Mts (38°N, 108°W), Dasuopu (28°N, 85°E) (Thompson et al. 2000), Kilimanjaro (3°S, 37°E) (Thompson et al. 2002), Huascaran (9°S, 77°W) (Thompson et al. 1995), Quelccaya (13°S, 70°W) (Thompson et al. 1984), James Ross Island (64°S, 58°W), Siple Station (76°S, 84°W) (Mosley-Thompson et al. 1990), and Newall Glacier (77°S, 162°E) (Mayewski et al. 1995).

scenarios are equally consistent with available observational data (Luo et al. 2008), and provide the first evidence for an impact of pollution on the processing of iron. As an additional analysis from Luo et al. (2008), we include changes in atmospheric processing due to changing sulfur emissions in Scenario I (**Figure 16a**). Also shown in **Table 1** are ocean basin averages of the soluble iron deposition changes between current and preindustrial times based on these model simulations.

These results suggest that soluble iron inputs to the oceans may have increased by 50–800% over much of the ocean during the preindustrial to current time period. This ignores any change in dust over this time period, which is likely to dominate the global budget. Future impacts of industrial growth on iron inputs to the ocean are not well known at this time.

The interactions between humans, carbon dioxide, climate and dust are shown schematically in **Figure 17**, and highlight that there is a potential positive feedback loop between higher carbon dioxide, reducing desert dust area, reducing iron deposition to the oceans (which could contribute to lower ocean productivity), lower carbon dioxide uptake by the oceans, and thus higher carbon dioxide concentrations. In addition, ocean productivity may cause the emission of

Figure 16

Modeled estimates of increases in soluble iron deposition to oceans (current/preindustrial) based solely on changes in combustion sources of iron and sulfates, not including changes in desert dust for the three scenarios shown in **Figure 12** (from Luo et al. 2008).

**Human perturbations to atmospheric
iron deposition to oceans**
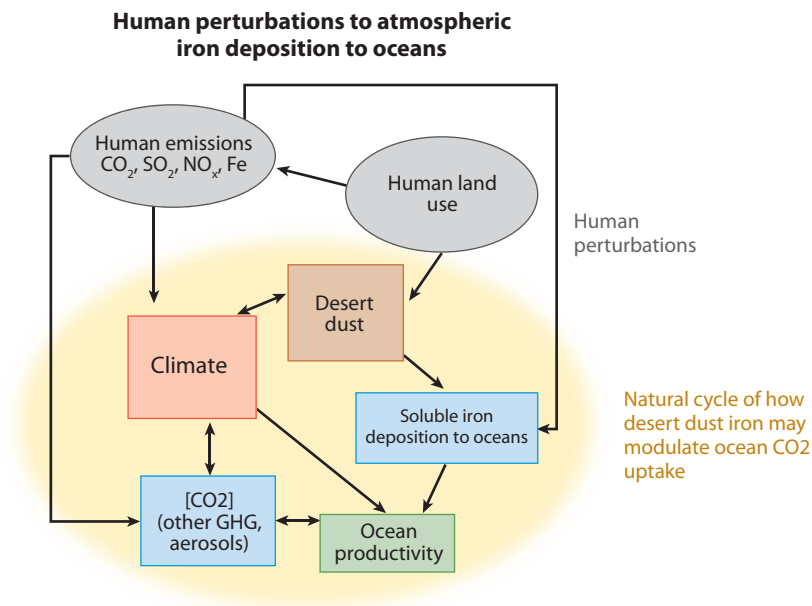
Figure 17

Schematic representing feedbacks between the natural ocean carbon cycle, carbon dioxide concentrations, and iron inputs; also shows how humans could be perturbing the iron deposition to the oceans.

other greenhouse gases (e.g., methane or nitrous oxide) or aerosols (sulfate or organic), thereby complicating this feedback (e.g., Jickells et al. 2005).

SUMMARY POINTS

1. Iron deposition to oceans is dominated by mineral aerosols, with 5% coming from combustion sources. Thus, the largest deposition of iron occurs downwind of the main deserts of the globe (North Africa and the Middle East).

2. The solubility of iron may be driven by both direct emissions of soluble combustion particles and atmospheric processing of insoluble iron in clouds.

3. Humans may be increasing or decreasing atmospheric dust owing to land use and climate change. Studies suggest large changes are possible $(+/-50\%)$.

4. Humans may be increasing soluble iron deposition to the oceans through increases in acidity of the atmosphere, which may increase atmospheric processing, or through increases in direct emissions of soluble iron in combustion. Studies suggest large changes are possible $(+100\%)$.

FUTURE ISSUES

1. The bioavailable iron speciation is not well known. It is unclear how biota extract iron from atmospheric deposition, and what fraction is bioavailable.

2. Assuming we know what portion of the iron is bioavailable, we need to measure that fraction in the atmosphere to better understand the sources and processes of bioavailable iron inputs to the oceans. We need a consistent measurement technique for the bioavailable fraction.

3. Iron and dust deposition are rarely measured directly and need to be measured more often.

4. Long-term measurements of iron, soluble iron, and dust concentration and deposition are required to understand the interannual and decadal variability of dust and iron and the weather and climate factors that may effect this variability.

5. We require more paleorecords of the changes in dust and iron transport over the past 200–1000 years to understand the natural variability of dust and to better quantify human impacts on dust mobilization.

6. We need to have a better understanding of the environmental characteristics of present-day dust sources and the factors that affect dust mobilization from these sources. It is especially important to focus on dust hotspots because they seem to be a major source of global-scale dust transports.

7. Research programs that focus on atmospheric dust should be more closely integrated with those that focus on ocean dust processes. Much of the present-day research in these fields is decoupled. Consequently, it is difficult to link the results of such studies in a meaningful way so as to bridge the ocean-atmosphere interface and yield a more quantitative understanding of the impact of global-scale dust processes on ocean biogeochemistry.

8. The performance of dust models needs to be further improved to reduce uncertainties in the estimates of dust and iron distributions, their response to humans, and their impacts. This is especially true for the soluble/bioavailable iron fraction.

DISCLOSURE STATEMENT

The authors are not aware of any biases that might be perceived as affecting the objectivity of this review.

ACKNOWLEDGMENTS

LITERATURE CITED

Baker A, Jickells T. 2006. Mineral particle size as a control on aerosol iron solubility. *Geophys. Res. Lett.* 33:L17608

Baker A, Jickells TD, Linge K. 2006a. Trends in the solubility of iron, aluminum, manganese and phosphorus in aerosol collected over the Atlantic Ocean. *Mar. Chem.* 98:43–58

Baker AR, French M, Linge KL. 2006b. Trends in aerosol nutrient solubility along a west-east transect of the Saharan dust plume. *Geophys. Res. Lett.* 33:L07805

Balkanski Y, Schulz M, Claquin T, Guibert S. 2007. Reevaluation of mineral aerosol radiative forcings suggests a better agreement with satellite and AERONET data. *Atmos. Chem. Phys.* 7:81–95

Barbeau K, Rue E, Bruland K, Butler A. 2001. Photochemical cycling of iron in the surface ocean mediated by microbial iron (III)-binding ligands. *Nature* 413:409–13

Bergquist B, Boyle E. 2006. Dissolved iron, manganese and chromium in the tropical and subtropical Atlantic ocean. *Glob. Biogeochem. Cycles* 20:GB1015

Bergquist B, Wu J, Boyle E. 2007. Variability in oceanic dissolved iron is dominated by the colloidal fraction. *Geochem. Cosmochim. Acta* 71:60–74

Bonnet S, Guieu C. 2004. Dissolution of atmospheric iron in seawater. *Geophys. Res. Lett.* 31:L03303

Bonnet S, Guieu C. 2006. Atmospheric forcing on the annual iron cycle in western Mediterranean Sea: a 1-year survey. *J. Geophys. Res.* 111:C09010

Bory A, Dulac F, Moulin C, Chiapello I, Newton P, et al. 2002. Atmospheric and oceanic dust fluxes in northeastern tropical Atlantic Ocean: How close a coupling? *Ann. Geophys.* 20:2067–76

Bory AJ-M, Biscaye PE, Grousset FE. 2003. Two distinct seasonal Asian source regions for mineral dust deposited in Greenland (North GRIP). *Geophys. Res. Lett.* 30:1167

Bory AJ-M, Newton PP. 2000. Transport of airborne lithogenic material down through the water column in two contrasting regions of the eastern subtropical North Atlantic Ocean. *Glob. Biogeochem. Cycles* 14:297–315

Boyle E, Bergquist B, Kayser R, Mahowald N. 2005. Iron, manganese and lead at Hawaii Ocean Time-Series Station ALOHA: temporal variability and intermediate water hydrothermal plume. *Geochim. Cosmochim. Acta* 69:933–52

Bryant R, Bigg G, Mahowald N, Eckhardt F, Ross S. 2007. Dust emission response to climate in southern Africa. *J. Geophys. Res.* 112:D09207

Cahill TA, Gill TE, Reid JS, Gearhart EA, Gillette DA. 1996. Salting particles, playa crusts and dust aerosols at Owens (dry) Lake, California. *Earth Surf. Process. Landf.* 21:621–39

Cakmur RV, Miller R, Tegen I. 2001. A comparison of seasonal and interannual variability of soil dust aerosols over the Atlantic Ocean as inferred by the TOMS AI and AVHRR AOT retrievals. *J. Geophys. Res.* 106:18287–303

Charney J, Quirk WJ, Chow S-H, Kornfield J. 1977. A comparative study of the effects of albedo change on rrought in semi-arid regions. *J. Atmos. Sci.* 34:1366–85

Chase Z, Paytan A, Johnson KS, Street J, Chen Y. 2006. Input and cycling of iron in the Gulf of Aqaba, Red Sea. *Glob. Biogeochem. Cycles* 20:GB3017

Chen Y, Mills S, Street J, Golan D, Post A, et al. 2007. Estimates of atmospheric dry deposition and associated input of nutrients to Gulf of Aqaba seawater. *J. Geophys. Res.* 112:D04309

Chen Y, Street J, Paytan A. 2006. Comparison between pure-water and seawater-soluble nutrient concentrations of aerosols from the Gulf of Aqaba. *Mar. Chem.* 101:141–52

Chen M, Xie P, Janowiak J, Arkin P. 2002. Global land precipitation: a 50-year monthly analysis based on gauge observations. *J. Hydrometeorol.* 3:249–66

Chuang P, Duvall R, Shafer M, Schauer J. 2005. The origin of water soluble particulate iron in the Asian atmospheric outflow. *Geophys. Res. Lett.* 32:L07813

Claquin T, Schulz M, Balkanski Y. 1999. Modeling the mineralogy of atmospheric dust sources. *J. Geophys. Res.* 104:22,243–56

D'Almeida GA. 1986. A model for Saharan dust transport. *J. Clim. Appl. Meteorol.* 25:903–16

Dai A, Trenberth K, Qian T. 2004. A global dataset of Palmer Drought Severity Index for 1870–2002: relationship with soil moisture and the effects of surface warming. *J. Hydrometeorol.* 5:1117–30

deMenocal P, Ortiz J, Guilderson T, Adkins J, Sarnthein M, et al. 2000. Abrupt onset and termination of the African Humid Period: rapid climate responses to gradual insolation forcing. *Quat. Sci. Rev.* 19:347–61

Denman K, Brassuer G, et al. 2007. Couplings between changes in the climate system and biogeochemistry. In *Climate Change 2007: The Physical Science Basis. Contribution of Working Group 1 to the Fourth Assessment*, ed. DQS Solomon, M Manning, Z Chen, M Marquis, KB Averyt, M Tignor, HL Miller. Cambridge, UK: Cambridge Univ. Press

Deutsch C, Sarmiento J, Sigman D, Gruber N, Dunne J. 2007. Spatial coupling of nitrogen inputs and losses in the ocean. *Nature* 445:163–67

Donarummo J, Ram M, Stolz MR. 2002. Sun/dust correlations and volcanic interference. *Geophys. Res. Lett.* 29:1361

Duce RA, Tindale NW. 1991. Atmospheric transport of iron and its deposition in the ocean. *Limnolog. Oceanogr.* 36:1715–26

Duggen S, Croot P, Schacht U, Hoffmann L. 2007. Subduction zone volcanic ash can fertilize the surfac eocean and stimulate phytoplankton growth: evidence from biogeochemical experiments and satellite data. *Geophys. Res. Lett.* 34:L01612

Dulac F, Bergametti G, Losno R, Remoudaki E, Gomes L, et al. 1992. Dry deposition of mineral aerosol partices in the marine atmosphere: significance of the large size fraction. In *Precipitation Scavenging and Atmosphere-Surface Exchange*, ed. SE Schwartz, WGN Slinn, pp. 841–54. Richland, WA: Hemisphere

Dulac F, Moulin C, Lambert C, Guillard F, Poitou J, et al. 1996. Quantative remote sensing of African dust transport to the Mediterranean. See Guerzoni & Chester 1996. pp. 25–49

Edwards R, Sedwick P. 2001. Iron in East Antarctic snow: implications for atmospheric iron deposition and algal production in Antarctic waters. *Geophys. Res. Lett.* 28:3907–10

Engelstaedter S, Kohfeld KE, Tegen I, Harrison SP. 2003. Controls of dust emissions by vegetation and topographic depressions: an evaluation using dust storm frequency data. *Geophys. Res. Lett.* 30:1294

Engelstaedter S, Washington R. 2007. Temporal controls on global dust emissions: the role of surface gustiness. *Geophys. Res. Lett.* 34:L15805

Falkowski PG, Barber RT, Smetacek V. 1998. Biogeochemical controls and feedbacks on ocean primary production. *Science* 281:200–6

Fan S-M, Moxim W, Levy H. 2006. Aeolian input of bioavailable iron to the ocean. *Geophys. Res. Lett.* 33:L07602

Foret G, Bergametti G, Dulac F, Menut L. 2006. An optimized particle size bin scheme for modeling mineral dust aerosol. *J. Geophys. Res.* 111:D17310

Francois R, Honjo S, Krishfield R, S. M. 2002. Factors controlling the flux of organic carbon to the bathypelagic zone of the ocean. *Glob. Biogeochem. Cycles* 16:1087

Frogner P, Gislason SR, Oskarsson N. 2001. Fertilizing potential of volcanic ash in ocean surface water. *Geol. Soc. Am.* 29:487–90

Fung I, Meyn SK, Tegen I, Doney S, John J, Bishop J. 2000. Iron supply and demand in the upper ocean. *Glob. Biogeochem. Cycles* 14:281–95

Gehlen M, Heinze C, Maier-Reimer E, Measures C. 2003. Coupled Al-Si geochemistry in an ocean general circulation model: a tool for the validation of oceanic dust deposition fields? *Glob. Biogeochem. Cycles* 17:1028

Giannini A, Saravanan R, Chang P. 2003. Oceanic forcing of Sahel rainfall on interannual to interdecadal time scales. *Science* 302:1027–30

Gill T. 1996. Eolian sediments generated by anthropogenic disturbance of playas: human impacts on the geomorphic system and geomorphic impacts on the human system. *Geomorphology* 17:207–28

Gillette DA. 1988. Threshold friction velocities for dust production for agricultural soils. *J. Geophys. Res.* 93:12645–62

Gillette DA. 1999. A qualitative geophysical explanation for "Hot Spot" dust emitting source regions. *Atmos. Phys.* 72:67–77

Ginoux P, Chin M, Tegen I, Prospero JM, Holben BN, et al. 2001. Sources and distribution of dust aerosols with the GOCART model. *J. Geophys. Res.* 106:20255–73

Ginoux P, Prospero JM, Torres O, Chin M. 2004. Long-term simulation of global dust distribution with the GOCART model: correlation with the North Atlantic Oscillation. *Environ. Model. Softw.* 19:113–28

Grousset F, Biscaye P. 2005. Tracing dust sources and transport partterns using Sr, Nd and Pb isotopes. *Chem. Geol.* 222:149–67

Grousset FE, Ginoux P, Bory A, Biscaye PE. 2003. Case study of a chinese dust plume reaching the French Alps. *Geophys. Res. Lett.* 30:1277

Guerzoni S, Chester R, ed. *The Impact of Desert Dust Across the Mediterranean*. Kluver Academic Publishers: Netherlands. 406 pp.

Guerzoni S, Molinaroli E, Chester R. 1997. Saharan dust inputs to the western Mediterranean Sea: depositional patterns, geochemistry and sedimentological implications. *Deep-Sea Res. II* 44:631–54

Guieu C, Bonnet S, Wagener T, Loye-Pilot M-D. 2005. Biomass burning as a source of dissolved iron to the open ocean? *Geophys. Res. Lett.* 32:L19608

Han Q, Moore JK, Zender C, Measures C. 2008. Constraining oceanic dust deposition using surface ocean dissolved Al. *Glob. Biogeochem. Cycles* 22:GB2003

Hand J, Mahowald N, Chen Y, Siefert R, Luo C, et al. 2004. Estimates of soluble iron from observations and a global mineral aerosol model: biogeochemical implications. *J. Geophys. Res.* 109:D17205

Herman JR, Bhartia PK, Torres O, Hsu C, Seftor C, Celarier E. 1997. Global distribution of UV-absorbing aerosols from Nimbus 7/TOMS data. *J. Geophys. Res.* 102:16911–22

Hoerling M, Hurrell J, Eischeid J, Phillips A. 2006. Detection and attribution of 20th century northern and southern African rainfall change. *J. Clim.* 19:3989–4008

Holben BN, Tanre D, Smirnov A, Eek TF, Slutsker I, et al. 2001. An emerging ground-based aerosol climatology:Aerosol optical depth from AERONET. *J. Geophys. Res.* 106:12067–97

Hurrell JW, Kushner Y, Visbeck M. 2001. The North Atlantic Oscillation. *Science* 291:603–5

Husar RB, Prospero JM, Stowe LL. 1997. Characterization of tropospheric aerosols over the oceans with the NOAA advanced very high resolution radiometer optical thickness operational product. *J. Geophys. Res.* 102:16889–909

Jickells T, An Z, Andersen K, Baker A, Bergametti G, et al. 2005. Global iron connections between dust, ocean biogeochemistry and climate. *Science* 308:67–71

Jickells T, Spokes L. 2001. Atmospheric iron inputs to the oceans. In *Biogeochemistry of Iron in Seawater*, ed. DR Turner, K Hunteger, pp. 85–121. Chichester: John Wiley and Sons, Ltd.

Jickells TD, Dorling S, Deuser WG, Church TM, Arimoto R, Prospero JM. 1998. Air-borne dust fluxes to a deep water sediment trap in the Sargasso Sea. *Glob. Biogeochem. Cycles* 12:311–20

Johansen AM, Siefert RL, Hoffmann MR. 2000. Chemical composition of aerosols collected over the tropical North Atlantic Ocean. *J. Geophys. Res.* 105:15277–312

Johansen AM, Key JM. 2006. Photoreductive dissolution of ferrihydrite by methanesulfinic acid: evidence of a direct link between dimethylsulfide and iron-bioavailability. *Geophys. Res. Lett.* 33:L14818

Johnson K. 2001. Iron supply and demand in the upper ocean: Is extraterrestrial dust a significant source of bioavailable iron? *Glob. Biogeochem. Cycles* 15:61–63

Johnson K, Boye E, Bruland K, Coale K, Measures C, et al. 2007. Developing standards for dissolved iron in seawater. *EOS* 88:131–32

Jones D, Mahowald N, Luo C. 2003. The role of easterly waves on African desert dust transport. *J. Clim.* 16:3617–2628

Journet E, Desboeufs K, Caquineau S, Colin J-L. 2008. Mineralogy as a critical factor of dust iron solubility. *Geophys. Res. Lett.* 35:L07805

Kieber R, Wiley J, Avery G. 2003. Temporal variability of rainwater iron speciation at the Bermuda Atlantic time series stations. *J. Geophys. Res.* 108:3277

Kieber R, Williams K, Wiley J, Skrabal S, Avery G. 2001. Iron speciation in coastal rainwater: concentration and deposition to seawater. *Mar. Chem.* 73:83–95

Kohfeld KE, Harrison SP. 2001. DIRTMAP: the geological record of dust. *Earth Sci. Rev.* 54:81–114

Kubilay N, Nickovic S, Moulin C, Dulac F. 2000. An illustration of the transport and deposition of mineral dust onto the eastern Mediterranean. *Atmos. Environ.* 34:1293–303

Lam P, Bishop J, Henning C, Marcus M, Waychunas G, Fung I. 2006. Wintertime phytoplankton bloom in the subarctic Pacific supported by continental margin iron. *Glob. Biogeochem. Cycles* 20:GB1006

Loye-Pilot M, Martin J, Morelli J. 1986. Influence of Saharan dust on the rain acidity and atmospheric input to the Mediterranean. *Nature* 321:427–28

Luo C, Mahowald N, Bond T, Chuang P, Artaxo P, et al. 2008. Combustion iron distribution and deposition. *Glob. Biogeochem. Cycles* 22:GB1012

Luo C, Mahowald N, del Corral J. 2003. Sensitivity study of meteorological parameters on mineral aerosol mobilization, transport and distribution. *J. Geophys. Res.* 108:4447

Luo C, Mahowald N, Jones C. 2004. Temporal variability of dust mobilization and concentration in source regions. *J. Geophys. Res.* 109:D20202

Luo C, Mahowald N, Meskihidze N, Chen Y, Siefert R, et al. 2005. Estimation of iron solubility from observations and a global aerosol model. *J. Geophys. Res.* 110:D23307

Mackie D, Boyd P, Hunter K, McTainsh G. 2005. Simulating the cloud processing of iron in Australian dust: pH and dust concentration. *Geophys. Res. Lett.* 32:L06809

Mahaffrey C, Williams R, Wolff G, Mahowald N, Anderson W, Woodward M. 2003. Biogeochemical signatures of nitrogen fixation in the eastern North Atlantic. *Geophys. Res. Lett.* 40:1300

Mahowald N. 2007. Anthropocene changes in desert area: sensitivity to climate model predictions. *Geophys. Res. Lett.* 34:L18817

Mahowald N, Baker A, Bergametti G, Brooks N, Duce R, et al. 2005. The atmospheric global dust cycle and iron inputs to the ocean. *Glob. Biogeochem. Cycles* 19:GB4025

Mahowald N, Ballentine J-A, Feddema J, Ramankutty N. 2007. Global trends in visibility: implications for dust sources. *Atmos. Chem. Phys.* 7:3013

Mahowald N, Muhs D, Levis S, Rasch P, Yoshioka M, Zender C. 2006. Change in atmospheric mineral aerosols in response to climate: last glacial period, preindustrial, modern and doubled-carbon dioxide climates. *J. Geophys. Res.* 111:D10202

Mahowald N, Dufresne J-L. 2004. Sensitivity of TOMS aerosol index to boundary layer height: implications for detection of mineral aerosol sources. *Geophys. Res. Lett.* 31:L03103

Mahowald N, Kohfeld K, Hansson M, Balkanski Y, Harrison SP, et al. 1999. Dust sources and deposition during the last glacial maximum and current climate: a comparison of model results with paleodata from ice cores and marine sediments. *J. Geophys. Res.* 104:15895–916

Mahowald N, Luo C, Corral Jd, Zender C. 2003. Interannual variability in atmospheric mineral aerosols from a 22-year model simulation and observational data. *J. Geophys. Res.* 108:4352

Mahowald N, Rivera G, Luo C. 2004. Comment on "Relative importance of climate and land use in determining present and future global soil dust emission." *Geophys. Res. Lett.* 31:L24105

Mahowald N, Zender C, Luo C, Corral Jd, Savoie D, Torres O. 2002. Understanding the 30-year Barbados desert dust record. *J. Geophys. Res.* 107:4561

Mahowald NM, Luo C. 2003. A less dusty future? *Geophys. Res. Lett.* 30:1903

Marticorena B, Bergametti G. 1995. Modeling the atmospheric dust cycle: 1. Design of a soil-derived dust emission scheme. *J. Geophys. Res.* 100:16415–30

Martin JH. 1990. Glacial-interglacial CO_2 change: the iron hypothesis. *Paleoceanography* 5:1–13

Mayewski PA, et al. 1995. An ice-core based late Holocene history for the transantarctic mountains, Antarctica. *Contrib. Antarctic Res. IV, Antarctic Res. Series* 67:33–45

Mbourou GNT, Bertrand JJ, Nicholson SE. 1997. The diurnal and seasonal cycles of wind-borne dust over Africa North of the equator. *J. Appl. Meteorol.* 36:868–82

McConnell JR, Aristarain A, Banta J, Edwards P, Simoes J. 2007. 20th Century doubling in dust archived in an Antarctic penisula ice core parallels climate change and desertification in South America. *Proc. Natl. Acad. Sci.* 104:5743–48

Measures C, Brown E. 1996. Estimating dust input to the Atlantic Ocean using surface water Al concentrations. See Guerzoni & Chester 1996. pp. 301–11

Meskhidze N, Chameides W, Nenes A. 2005. Dust and pollution: A recipe for enhanced ocean fertilization? *J. Geophys. Res.* 110:D03301

Meskhidze N, Chameides WL, Nenes A, Chen G. 2003. Iron mobilization in mineral dust: Can anthropogenic SO_2 emissions affect ocean productivity? *Geophys. Res. Lett.* 30:2085

Micklin PP. 1988. Dessication of the Aral Sea: a water management disaster in the Soviet Union. *Science* 241:1170–76

Middleton N, Betzer P, Bull P. 2001. Long-range transport of 'giant' aeolian quartz grains: linkage with discrete sedimentary sources and implications for protective particle transfer. *Marine Geol.* 177:411–17

Miller R, Cakmur R, Perlwitz J, Geogdzhayev I, Ginoux P, et al. 2006. Mineral dust aerosols in the NASA Goddard Institute of Space Sciences ModelE Atmospheric General Circulation Model. *J. Geophys. Res.* 111:D06208

Miller R, Tegen I, Perlwitz J. 2004. Surface radiative forcing by soil dust aerosols and the hydrologic cycle. *J. Geophys. Res.* 109:D04203

Mills MM, Ridame C, Davey M, LaRoche J, Geider R. 2004. Iron and phosphorus colimit nitrogen fixation in the eastern tropical North Atlantic. *Nature* 429:292–94

Moore JK, Doney SC, Lindsay K. 2004. Upper ocean ecosystem dynamics and iron cycling in a global three-dimensional model. *Glob. Biogeochem. Cycles* 18:GB4028

Mosley-Thompson E, Thompson LG, Grootes P, Gundestrup N. 1990. Little ice age (neoglacial) paleoenvironmental conditions at Siple station, Antarctica. *J. Glaciol.* 14:199–204

Moulin C, Lambert CE, Dulac F, Dayan U. 1997a. Control of atmospheric export of dust from North Africa by the North Atlantic Oscillation. *Nature* 387:691–4

Moulin C, Guillard F, Dulac F, Lambert CE. 1997b. Long-term daily monitoring of Saharan dust load over ocean using ISCCP-B2 data. 2. Accuracy of the method and validation using Sun photometer measurements. *J. Geophys. Res.* 102:16959–69

Moulin C, Chiapello I. 2006. Impact of human-induced desertification on the intensification of the Sahel dust emission and export over the last decades. *Geophys. Res. Lett.* 33:L18808

Neff J, Ballantine A, Farmer G, Mahowald N, Conroy J, et al. 2008. Increasing eolian dust deposition in the western United States linked to human activity. *Nat. Geosci.* 1:189–95

Neff J, Reynolds R, Belnap J, Lamothe P. 2005. Multi-decadal impacts of grazing on soil physical and biogeochemical properties in southeast Utah. *Ecol. Appl.* 15:87–95

Ozsoy T, Saydam A. 2001. Iron speciation in precipitation in the North-eastern Mediterranean and its relationship with Sahara dust. *J. Atmos. Chem.* 40:41–76

Parekh P, Follows M, Boyle E. 2004. Modeling the global ocean iron cycle. *Glob. Biogeochem. Cycles* 18:GB1002

Patra P, Kumar MD, Mahowald N, Sarma V. 2007. Atmospheric deposition and surface stratification as controls of contrasting chlorophyll abundance in the North Indian Ocean. *J. Geophys. Res.* 112:C05029

Prospero J. 2006. *Long term records of dust transport over the North Atlantic Ocean: an overview*. Presented at Am. Geophys. Union Fall Meet.

Prospero J. 2007. *Long-term measurements of African dust deposition across the state of Florida: How well do models do?* Presented at Int. Union Geod. Geophys. Meeting

Prospero J, Ginoux P, Torres O, Nicholson SE. 2002. Environmental characterization of global sources of atmospheric soil dust derived from the NIMBUS-7 TOMS absorbing aerosol product. *Rev. Geophys.* 40:1002

Prospero J, Lamb P. 2003. African droughts and dust transport to the Caribbean: climate change implications. *Science* 302:1024–27.

Prospero JM. 1996. Saharan dust transport over the North Atlantic Ocean and Mediterranean: an overview. See Guerzoni & Chester 1996. pp. 133–151

Prospero JM. 1999. Long-range transport of mineral dust in the global atmosphere: impact of African dust on the environment of the southeastern United States. *Proc. Natl. Acad. Sci.* 96:3396–403

Prospero JM, Bonatti E. 1969. Continental dust in the atmosphere of the eastern equatorial pacific. *J. Geophys. Res.* 74:3362–71

Prospero JM, Nees RT. 1986. Impact of the North African drought and El Niño on mineral dust in the Barbados trade winds. *Nature* 320:735–38

Prospero JM, Nees RT, Uematsu M. 1987. Deposition rate of particulate and dissolved aluminum derived from Saharan dust in precipitation at Miami, Florida. *J. Geophys Res.* 92:14723–31

Rasch PJ, Collins W, Eaton BE. 2001. Understanding the Indian ocean experiment (INDOEX) aerosol distributions with an aerosol assimilation. *J. Geophys. Res.* 106:7337–55

Rasch PJ, Feichter H, Law K, Mahowald N, Penner J, et al. 2000. An assessment of scavenging and deposition processes in global models: results from the WCRP Cambridge workshop of 1995. *Tellus* 52B:1025–56

Redemann J, Zhsang Q, Schmid B, Russel P, Livingston J, et al. 2006. Assessment of MODIS-derived visible and near-IR aerosol optical properties and their spatial variability in the presence of mineral dust. *Geophys. Res. Lett.* 33:L18814

Reid E, Reid J, Meier M, Dunlap M, Cliff S, et al. 2003. Characterization of African dust transported to Puerto Rico by individual particle and size segregated bulk analysis. *J. Geophys. Res.* 108:8591

Remer L, Kaufman Y, Tanre D, Mattoo S, Chu D, et al. 2005. The MODIS aerosol algorithm, products and validation. *J. Atmos. Sci.* 62:947–73

Ridame C, Guieu C, Loye-Pilo M-D. 1999. Trend in total atmospheric deposition fluxes of aluminium, iron and trace metals in the northwestern Mediterranean over the past decade (1985–1997). *J. Geophys. Res.* 104:30127–38

Ridgwell AJ, Watson AJ. 2002. Feedback between aeolian dust, climate and atmospheric CO_2 in glacial time. *Paleoceanography* 17:1059

Rostayn L, Lohman U. 2002. Tropical rainfall trends and the indirect aerosols effect. *J. Clim.* 15:2103–16

Saydam AC, Senyuva HZ. 2002. Deserts: Can they be the potential suppliers of bioavailable iron? *Geophys. Res. Lett.* 29:1524

Schepanski K, Tegen I, Laurent B, Heinold B, Macke A. 2007. A new Saharan dust source activiation frequency map derived from MSG-SEVIRI IR-channels. *Geophys. Res. Lett.* 34:L18803

Sedwick P, Sholkovitz E, Church T. 2007. Impact of anthropogenic combustion emissions on the fractional solubility of aerosol iron: evidence from the Sargasso Sea. *Geochem. Geophys. Geosyst.* 8:Q10Q06

Seinfeld JH, Pandis SN. 1998. *Atmospheric Chemistry and Physics*. New York: John Wiley and Sons, Inc. 1326 pp.

Siefert R, Johansen A, Hoffman M. 1999. Chemical characterization of ambient aerosol collected during the southwest monsoon and intermonsoon seasons over the Arabian Sea: labile-Fe(II) and other trace metals. *J. Geophys. Res.* 104:3511–26

Siegel DA, Deuser WG. 1997. Trajectories of sinking particles in the Sargasso Sea: modeling of statistical funnels above deep-ocean sediment traps. *Deep-Sea Res.* 44:1519–41

Smith S, Huxman T, Zitzer S, Charlet T, Housman D, et al. 2000. Elevated CO_2 increases productivity and invasive species success in an arid ecosystem. *Nature* 408:79–82

Smith SJ, Conception E, Andres R, Lurz J. 2004. Historical sulfur dioxide emissions, 1850–2000: methods and results. *Rep. PNNL-14537*, Richland WA: Pacific Northwest National Lab

Tanaka T, Chiba M. 2006. A numerical study of the contributions of dust source regions to the global dust budget. *Glob. Planet. Chang.* 52:88–104

Tanré D, Kaufman YJ, Herman M, Mattoo S. 1997. Remote sensing of aerosol properties over oceans using the MODIS/EOS spectral radiances. *J. Geophys. Res.* 102:16971–88

Taylor SR, McLennan SM. 1985. *The Continental Crust: Its Composition and Evolution*. Oxford: Blackwell Scientific Publishing, 312 pp.

Tegen I. 2003. Modeling the mineral dust aerosol cycle in the climate system. *Quarternary Sci. Rev.* 22:1821–34

Tegen I, Fung I. 1994. Modeling of mineral dust in the atmosphere: sources, transport, and optical thickness. *J. Geophys. Res.* 99:22897–914

Tegen I, Harrison SP, Kohfeld K, Prentice C, Coe M, Heimann M. 2002. The impact of vegetation and preferential source areas on global dust aerosol: results from a model study. *J. Geophys. Res.* 107:4576

Tegen I, Hollrig P, Chin M, Fung I, Jacob D, Penner J. 1997. Contribution of different aerosol species to the global aerosol extinction optical thickness: estimates from model results. *J. Geophys. Res.* 102:23895–915

Tegen I, Werner M, Harrison SP, Kohfeld KE. 2004. Relative importance of climate and land use in determining present and future global soil dust emission. *Geophys. Res. Lett.* 31:L05105

Textor C, Schulz1 M, Guibert S, Kinne S, Balkanski Y, et al. 2006. Analysis and quantification of the diversities of aerosol life cycles within AeroCOM. *Atmos. Chem. Phys.* 6:1777–813

Thompson LG, Mosley-Thompson E, Davis M, Henderson K, Brecher HH, et al. 2002. Kilimanjaro ice core records: evidence of Holocene climate change in tropical Africa. *Science* 298:589–93

Thompson LG, Mosley-Thompson E, Davis ME, Lin P-N, Henderson KA, et al. 1995. Late glacial stage and Holocene tropical ice core records from Huascarán, Peru. *Science* 269:46–50

Thompson LG, Mosley-Thompson E, Grootes P, Pourchet M. 1984. Tropical glaciers: potential for paleoclimatic reconstruction. *J. Geophys. Res.* 89:4638–46

Thompson LG, Yao T, Mosley-Thomspon E, Davis ME, Henderson KA, Lin PN. 2000. A high-resolution millennial record of the South Asian monsoon from Himalayan ice cores. *Science* 289:1916–19

Times Atlas of the World. 1999, New York: Times Book Group, Ltd.

Torres O, Bhartia P, Herman J, Sinyuk A, Ginoux P, Holben B. 2002. A long-term record of aerosol optical depth from TOMS observations and comparison to AERONET measurements. *J. Atmos. Sci.* 59:398–431

Torres O, Bhartia PK, Herman JR, Ahmad Z, Gleason J. 1998. Derivation of aerosol properties from satellite measurements of backscattered UV radiation: theoretical basis. *J. Geophys. Res.* 103:17099–110

Visser F, Gerringa J, Gaast SVd, Baar Hd, Timmermans K. 2003. The role of the reactivity and content of iron of aerosol dust on growth rates of two Antarctic diatom species. *J. Phycol.* 29:1085–94

Wagener T, Guieu C, Losno R, Bonnet S, Mahowald N. 2008. Revisiting atmospheric dust export to the Southern Ocean: biogeochemical implications. *Glob. Biogeochem. Cycles* 22:GB2006

Warren A, Chappel A, Todd M, Bristol C, Drake N, et al. 2007. Dust riding in the dustiest place on Earth. *Geomorphology* 92:25–37

Washington R, Todd M, Middlleton N, Goudie A. 2003 Dust-storm source areas determined by the total ozone monitoring spectrometer and surface observations. *Ann. Assoc. Am. Geogr.* 93:297–313

Weber L, Wolker C, Schartau M, Wolf-Gladrow D. 2005. Modeling the speciation and biogeochemistry of iron at the Bermuda Atlantic Time-series Study site. *Glob. Biogeochem. Cycles* 19:GB1019

Winckler G, Anderson R, Fleischer M, McGee D, Mahowald N. 2008. Covariant glacial-interglacial dust fluxes in the equatorial Pacific. *Sci. Express* 320:93–96

Woodward S, Roberts D, Betts R. 2005. A simulation of the effect of climate change-induced desertification on mineral dust aerosol. *Geophys. Res. Lett.* 32:L18810

Xuan J, Sokolik I. 2002. Characterization of sources and emission rates of mineral dust in northern China. *Atmos. Environ.* 36:4863–76

Xue X, Shukla J. 1993. The influence of land surface properties on Sahel climate. Part I: desertification. *J. Clim.* 6:2232–45

Yoshioka M, Mahowald N, Conley A, Collins W, Fillmore D, Coleman D. 2007. Impact of desert dust radiative forcing on Sahel precipitation: relative importance of dust compared to sea surface temperature variations, vegetation changes and greenhouse gas warming. *J. Clim.* 20:1445–67

Yoshioka M, Mahowald N, Dufresne J-L, Luo C. 2005. Simulation of absorbing aerosol indices for African dust. *J. Geophys. Res.* 110:D18S17

Zdanowicz CM, Zielinski GA, Wake CP. 1998. Characteristics of modern atmospheric dust deposition in snow on the Penny ice cap, Baffin Island, Arctic Canada. *Tellus* 50B:506–20

Zender C, Bian H, Newman D. 2003. Mineral dust entrainment and deposition (DEAD) model: description and 1990s dust climatology. *J. Geophys. Res.* 108:4416

Zhang J, Christopher S. 2003. Long wave radiative forcing of Saharan dust aerosols estimated from MODIS, MISR and CERES observations on TERRA. *Geophys. Res. Lett.* 30:2188

Zhu X, Prospero JM, Millero FJ, Savoie DL, Brass GW. 1992. The solubility of ferric ion in marine mineral aerosol solutions at ambient relative humidities. *Mar. Chem.* 38:91–107

Zhu X, Prospero J, Millero F. 1997. Diel variability of soluble Fe(II) and soluble total Fe in North Africa dust in the trade winds at Barbados. *J. Geophys. Res.* 102:21297–305

Zhuang G, Yi Z, Duce RA, Brown PR. 1992. Chemistry of iron in marine aerosols. *Glob. Biogeochem. Cycles* 6:161–73

Zielinski GA, Mershon GR. 1997. Paleoenvironmental implications of insoluble microparticle record in the GISP2 (Greenland) ice core during the rapidly changing climate of the Pleistocene-Holocene transition. *Geol. Soc. Am. Bull.* 109:547–59